



ELSEVIER

Palaeogeography, Palaeoclimatology, Palaeoecology 199 (2003) 229–264

**PALAEO**

[www.elsevier.com/locate/palaeo](http://www.elsevier.com/locate/palaeo)

## Integrated stratigraphy and astronomical tuning of the Serravallian and lower Tortonian at Monte dei Corvi (Middle–Upper Miocene, northern Italy)

F.J. Hilgen<sup>a,\*</sup>, H. Abdul Aziz<sup>b</sup>, W. Krijgsman<sup>b</sup>, I. Raffi<sup>c</sup>, E. Turco<sup>d</sup>

<sup>a</sup> *IPPU, Utrecht University, Budapestlaan 4, 3584 CD Utrecht, The Netherlands*

<sup>b</sup> *Paleomagnetic Laboratory, Fort Hoofddijk, Budapestlaan 17, 3584 CD Utrecht, The Netherlands*

<sup>c</sup> *Dip. di Scienze della Terra, Univ. 'G. D'Annunzio', via dei Vestini 31, 66013 Chieti Scalo, Italy*

<sup>d</sup> *Dip. di Scienze della Terra, Università di Parma, Parco Area delle Scienze 157/A, 43100 Parma, Italy*

Received 3 October 2002; accepted 13 June 2003

### Abstract

An integrated stratigraphy (calcareous plankton biostratigraphy, magnetostratigraphy and cyclostratigraphy) is presented for the Serravallian and lower Tortonian part (Middle–Upper Miocene) of the Monte dei Corvi section located in northern Italy. The detailed biostratigraphic analysis showed that both the *Discoaster kugleri* acme and the first influx of *Neogloboquadrina acostaensis* are recorded at Monte dei Corvi; these events, which passed unobserved in previous studies, play an important role in delineating the Serravallian–Tortonian boundary. Thermal and alternating field demagnetization revealed a characteristic low-temperature component marked by dual polarities. The resultant magnetostratigraphy for the upper part of the section can be unambiguously calibrated to the GPTS ranging from C5n.2n up to C4r.2r. Unfortunately, the lower part of the section, including the Serravallian–Tortonian boundary interval, did not produce a reliable magnetostratigraphy despite the fact that some short reversed intervals and a single normal interval are recorded. Using sedimentary cycle patterns in combination with the calcareous plankton biostratigraphy the section can be correlated cyclostratigraphically in detail to the partially overlapping and previously tuned section of Monte Gibliscemi on Sicily. The Monte dei Corvi section is dated astronomically by calibrating the basic small-scale sedimentary cycles to the precession and 65°N lat. summer insolation time series of the La93 solution following an initial tuning of larger-scale cycles to eccentricity. An almost perfect fit is found between the cycle patterns and intricate details, especially precession–obliquity interference, in the insolation target between 8.5 and 10 Ma. The tuning to precession remains robust for most intervals back to the base of the section dated at 13.4 Ma and shows that the section is continuous apart from a possible short hiatus in the Tortonian. It provides accurate astronomical ages for all sedimentary cycles, calcareous plankton events, polarity reversals and ash layers and marks a significant improvement of the recently proposed astronomical calibrations of the Monte dei Corvi section and of parallel sections in the Mediterranean. Astronomical ages for the Ancona and Respighi ashbeds are significantly older than previously reported <sup>40</sup>Ar/<sup>39</sup>Ar biotite ages, even if the revised older age for the FCT-san dating standard of 28.02 Ma is applied. The astronomical dating of the magnetic reversals in the Monte dei Corvi section results in the completion of the astronomical polarity time scale for the last 13 Myr. The Monte dei Corvi section has recently been proposed as the stratotype section for the Serravallian–Tortonian boundary despite the moderate to

\* Corresponding author. Tel.: +31-30-2535173; Fax: +31-30-2535030.

E-mail address: [fhilgen@geo.uu.nl](mailto:fhilgen@geo.uu.nl) (F.J. Hilgen).

poor preservation of the calcareous microfossils and the lack of a reliable magnetostratigraphy across the boundary interval. Finally, our study reveals that a single dominantly precession controlled oscillatory climate system is responsible for late Neogene sapropel formation in the Mediterranean during the last 13.5 million years.

© 2003 Elsevier B.V. All rights reserved.

*Keywords:* astronomical time scale; biostratigraphy; magnetostratigraphy; cyclostratigraphy; chronostratigraphy; Neogene

---

## 1. Introduction

The Middle Miocene represents an intriguing period of time in the Earth's history during which the present-day ocean-climate system and continental configuration took shape. A detailed understanding of its history is limited, however, by the accuracy and resolution in dating sedimentary archives of that age. Recently climatostratigraphic criteria were used to obtain an astronomical calibration for marine cyclically bedded successions from Ceara Rise (Shackleton and Crowhurst, 1997) and the Mediterranean (Hilgen et al., 2000a; Cleaveland et al., 2002; Caruso et al., 2002; Lirer et al., 2002; Sprovieri et al., 2002a). The astronomical tuning for Ceara Rise has been extended back into the Oligocene (Shackleton et al., 1999) but details of the tuning of the Middle Miocene remain uncertain (Pälike and Shackleton, 2000). In the Mediterranean, the tuning has not been extended further back in time than 14 Ma and, in all cases, the lack of a reliable magnetostratigraphy prevents Middle Miocene astrochronology to be applied on a global scale.

A major research effort to improve temporal resolution and accuracy was further made by the Miocene Columbus Project (MICOP; Montanari et al., 1997a). This project was directed at improving the stratigraphy and chronology of the Miocene mainly by dating volcanic ash layers in marine pelagic successions with a good biostratigraphic control. Climatostratigraphic criteria were not applied in a systematic way and magnetostratigraphic data are either lacking or of a poor quality. One of the most important and intensively studied MICOP sections is Monte dei Corvi in northern Italy (Montanari et al., 1997b).  $^{40}\text{Ar}/^{39}\text{Ar}$  incremental heating experiments on biotites from two ash layers provided the necessary first-order age control (Montanari

et al., 1997b) and the section was proposed as a potential stratotype for the Serravallian, Tortonian and Messinian global stratotype sections and points (GSSPs) by Odin et al. (1997).

Recently, spectral analysis of a high-resolution carbonate record provided convincing evidence for an orbital control in the Monte dei Corvi section (Cleaveland et al., 2002) and an attempt was made to tune the low-frequency variations in carbonate content to the eccentricity time series within the constraints provided by the  $^{40}\text{Ar}/^{39}\text{Ar}$  biotite ages of the two ash layers. But the distinct small-scale cyclic bedding observed at Monte dei Corvi (Montanari et al., 1997b) suggests that the section is also suitable for astronomical tuning on the precession scale. Here we apply the high-resolution tuning method – fully integrated with magnetostratigraphy and calcareous plankton biostratigraphy – to the Serravallian and lower Tortonian part of the Monte dei Corvi composite as exposed in the beach section of Montanari et al. (1997b). The integrated approach is important because there is serious doubt about the continuity of the succession since neither the first neogloboquadrinid influx nor the *Discoaster kugleri* acme recorded at Monte Gibliscemi (Hilgen et al., 2000a) have thus far been found at Monte dei Corvi. Our main objectives are to establish an astronomical tuning to precession and insolation for the Monte dei Corvi Beach section, to test the tuning of the lower part of this section to eccentricity as proposed by Cleaveland et al. (2002) and of parallel sections located elsewhere in the Mediterranean (Caruso et al., 2002; Lirer et al., 2002; Sprovieri et al., 2002a), and to clarify the potential of Monte dei Corvi for defining the lower limit of the Tortonian Stage. Astronomical dating of the section will further contribute to the intercalibration of the astronomical and  $^{40}\text{Ar}/^{39}\text{Ar}$  radiometric dating methods by providing accurate

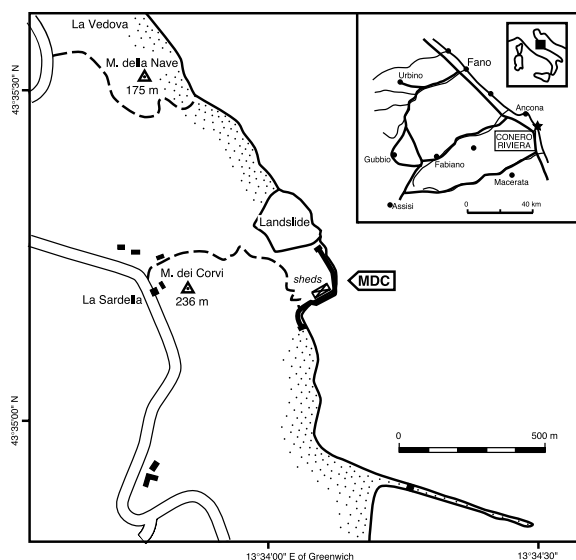


Fig. 1. Location and sample trajectory of the Monte dei Corvi section (MDC, after Montanari et al., 1997b).

precession ages for ash layers that have already been dated by  $^{40}\text{Ar}/^{39}\text{Ar}$  stepwise heating experiments on biotites.

## 2. Geological setting and section

The Miocene succession exposed in the coastal cliffs of the Conero Riviera south of Ancona in northern Italy (Fig. 1) is particularly suitable for integrated stratigraphic studies because it occupied a relatively external position with respect to the developing Apenninic orogen at that time (Montanari et al., 1997b). For this reason the succession remained pelagic throughout most of the Miocene, being affected by the NE-ward prograding orogenic front and associated flysch-like sedimentation at a late, post-Miocene stage. The entire succession extends from the Aquitanian into the Pliocene and contains the Bisciaro (Aquitanian to Langhian), Schlier (Langhian to Tortonian), Euxinic Shale and Gessoso Solifera (Messinian) formations of the northern Apennines (Montanari et al., 1997b).

In this paper we focus on the Serravallian and lower Tortonian part of the succession exposed along the eastern slopes and in the coastal cliffs

of Monte dei Corvi described in detail by Montanari et al. (1997b). This interval is particularly well exposed in the Monte dei Corvi Beach section of Montanari et al. (1997b), which is composed of a cyclic alternation of greenish-gray marls, whitish marly limestones and brown colored organic-rich layers (sapropels). In addition, two biotite-rich volcanic ash layers, named Respighi and Ancona, are present in this part of the succession which ranges from NN6 (MNN6b) to NN9 (MNN9) in terms of calcareous nannofossil biostratigraphy and from N11 to N16 in terms of planktonic foraminiferal biostratigraphy (Montanari et al., 1997b).

## 3. Cyclostratigraphy

The studied succession is composed of a cyclic alternation of marls, marly limestones and organic-rich beds (Montanari et al., 1997b). The basic small-scale cycle is a couplet (0.3–1.0 m thick) which consists of an indurated whitish marly limestone and a softer gray to greenish-gray marl (Fig. 2). Brownish to blackish colored organic-rich beds are often (but not always) intercalated in the limestones (Fig. 3). In the present paper, these beds are termed sapropels because they have the same origin as sapropels described from the younger part of the Mediterranean Neogene (this paper). They were named black shales by Montanari et al. (1997b). While logging the succession, a visual distinction was made between faint, visible, distinct and prominent sapropels. In doing so, serious problems were encountered due to weathering-induced lateral changes in (visual) distinctness of the sapropels. For this reason we decided to log that trajectory along which the sapropels are most clearly discernible. The most problematic interval starts some 5–10 m east of the fishermen's sheds, and includes the passage underneath the sheds itself. In practice, this part of the trajectory followed rocks exposed in the (present-day) intertidal zone. The visual expression of the sapropels rapidly diminishes or even disappears both in the subtidal realm as well as in the coastal cliffs in which more weathered rocks are exposed.

The position of a sapropel within a basic cycle

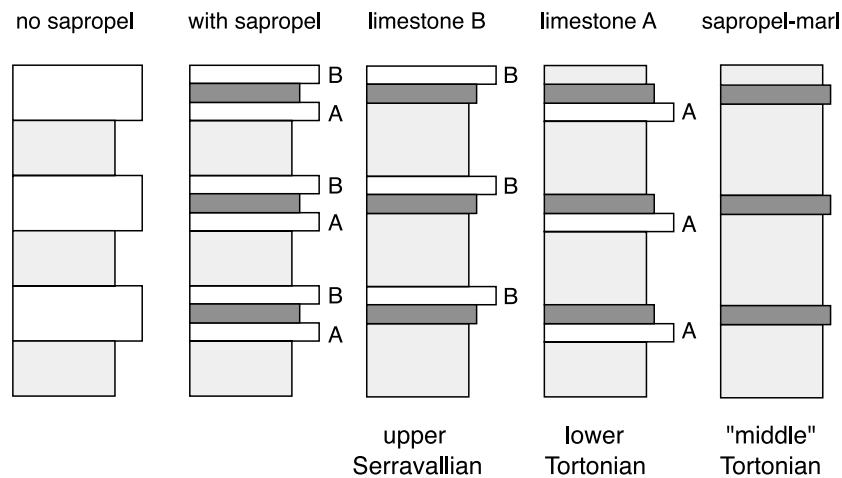


Fig. 2. Variations in the internal buildup of basic sedimentary cycles in the Monte dei Corvi section. The position of a sapropel within a basic cycle allows to distinguish between a lower (labelled A, below the sapropel) and an upper (B, above) limestone bed.

allows to distinguish between a lower (labelled A, below the sapropel) and an upper (B, above) limestone bed (Fig. 2). Bed A is not developed in most of the basic cycles in the lower part of the section. Basic cycles often lack bed B in the interval between 75 and 90 m, while they change into homogeneous marl-sapropel alternations in the top part of the section west of the fishermen's sheds (Figs. 2 and 3). The topmost part of this section, although logged in the more weathered cliffs, is excellently exposed along the waterfront. For an additional check on the basic cycle patterns, a short freshly exposed parallel section was uncovered across the beach by removing 50–100 cm thick loose pebbly beach deposits. The weathering profile of this parallel section reveals the presence of additional cycles as more indurated and protruding marly limestone beds in homogeneous marls that are extraordinarily thick (Fig. 4). Basic cycles have been labelled from the base of the section upward by assigning consecutive numbers to the limestone beds (A, B or AB undifferentiated) or the corresponding sapropels (Fig. 3). Two thick intervals labelled I and II occur in the middle part of the section in which the basic cyclicity could not be adequately resolved in the field.

At Monte dei Corvi, larger-scale cycles can be

distinguished in addition to the basic cycles and comprise both small-scale and large-scale sapropel clusters. These clusters are separated by intervals in which the basic small-scale cyclicity is usually still discernible but in which the brownish organic rich layers are generally absent. Sapropel clusters are distinctly present in the lower half and top part of the section, and are clearly manifested in case sapropels are separately depicted in a lithological column and if their visual distinctness is taken into account (Fig. 3). Small-scale clusters contain 2–4 sapropels (and 5–6 basic cycles); large-scale clusters contain several small-scale clusters (and up to 20 basic cycles) and have been labelled informally A to L. Finally, a cycle of intermediate scale is revealed by alternating thick/thin – or present/absent, or distinct/faint – sapropels in successive basic cycles. This intermediate cycle is particularly evident in two intervals (i.e. from cycle 38 to cycle 51 in the lower half of the section and from cycle 150 to cycle 176 in the upper half of the section). However, this cycle can also be recognized in other less thick intervals (i.e. cycles 201–203 and 136–145). Previous studies of marine sections of late Miocene to Pleistocene age in the Mediterranean (Hilgen, 1991a; Hilgen et al., 1995; Lourens et al., 1996) have shown that similar sapropel patterns reflect

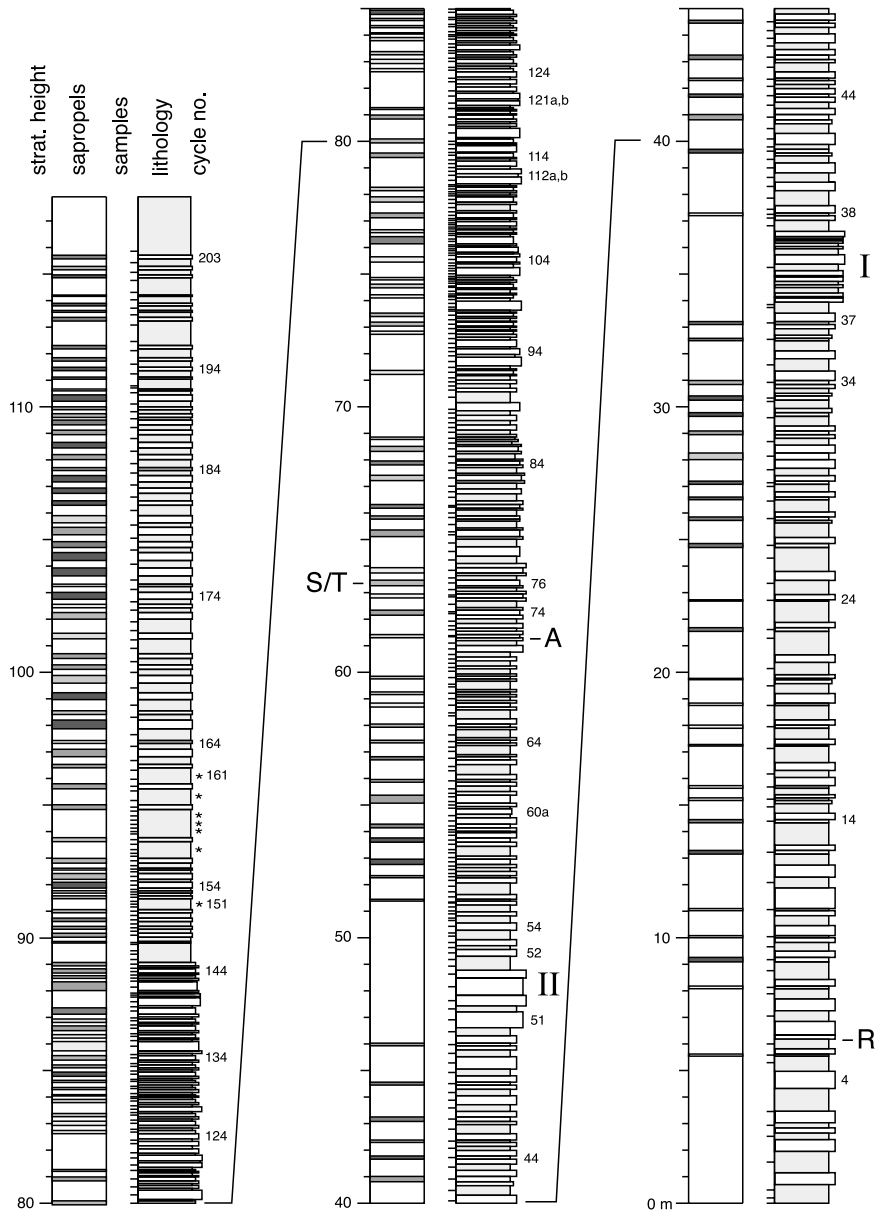


Fig. 3. Lithological column of the Monte dei Corvi section showing lithology, sample positions and cycle numbers. Grey shading in the lithological column marks the softer gray colored homogeneous marls. Whitish beds include both marly limestones and sapropels. Sapropels have been indicated in a separate column which reveals their visual distinctness, ranging from prominent (dark shading) via distinct and visible to faint (light shading) and very faint (no shading). Asterisks (\*) mark the position of poorly developed cycles observed in the Monte dei Corvi trench section across the beach (see also Fig. 4). A and R mark the position of the Ancona and Respighi ash layers, respectively. I and R indicate the thick intervals in which the basic small-scale cyclicity could not be adequately resolved.

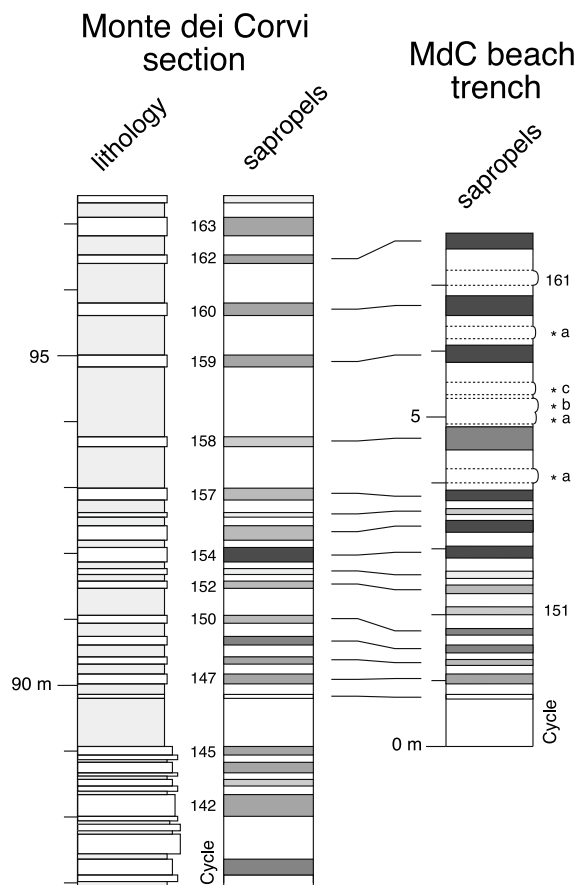


Fig. 4. Comparison of basic cycle patterns in the Monte dei Corvi trench section across the beach and the same interval in the regular Monte dei Corvi section exposed in the coastal cliffs.

the astronomical cycles of precession (basic cycle), obliquity (intermediate cycle) and eccentricity (larger-scale cycles).

#### 4. Calcareous plankton biostratigraphy

Our biostratigraphic analysis of the calcareous plankton (planktonic foraminifers and calcareous nannoplankton) focussed on the lower 93 m of the section (Fig. 5) because the biostratigraphy of the younger part has been well documented in time equivalent sections in the Mediterranean (Hilgen et al., 1995, 2000a,b,c; Raffi et al., 2003); these sections show a much better preservation

and can be perfectly correlated to Monte dei Corvi on the basis of the sedimentary cycle patterns.

##### 4.1. Planktonic foraminifera

Planktonic foraminiferal biostratigraphic studies of the Monte dei Corvi section have been carried out previously by Coccioni et al. (1992, 1994) and Montanari et al. (1997b). In these studies, all biohorizons of Mediterranean zonal schemes for the Serravallian–Tortonian (e.g. Iaccarino, 1985) were recognized, but the distribution patterns of the marker species were not presented. Our aim is (1) to refine and where necessary modify the existing planktonic foraminiferal biostratigraphy of the Monte dei Corvi Beach section by presenting the detailed distribution pattern of the main marker species, and (2) to compare the biostratigraphic results with those of other astronomically tuned sections in the Mediterranean, in particular the Monte Gibliscemi section (Hilgen et al., 2000a).

A semi-quantitative analysis was carried out on approximately 200 samples with an average resolution of 1–2 samples per small-scale sedimentary cycle. The sample resolution was higher in the interval between ~52 m and ~74 m in which most of the bioevents are located. The semi-quantitative analysis was based on surveying a standard number of fields (27 out of 45) in a rectangular picking tray while distinguishing the following abundance categories: Trace (< 3 specimens in 9 fields), Rare (3–10 specimens), Common (10–30 specimens), and Frequent (> 30 specimens). Preservation is generally poor, the planktonic foraminifera being strongly recrystallized and sometimes deformed and/or broken. Planktonic foraminifera are less abundant but show a better preservation in the sapropels than in the marl and limestone layers. Only a few sapropel samples are barren in foraminifera. The results of our semi-quantitative analysis are presented in Fig. 5. Taxonomy and distribution patterns are discussed below and compared with previous data from the Monte dei Corvi section (Montanari et al., 1997b) and, for the late Serravallian to early Tortonian, with data from the Monte Gibliscemi, Case Pelacani, San Nicola Is-

land and Ras il-Pellegrin sections (Hilgen et al., 2000a; Caruso et al., 2002; Foresi et al., 2002a,b). In Plate I the main marker species are depicted and compared to better preserved specimens from other Mediterranean sections (Monte Gibliscemi and Tremiti Islands). Although the preservation is rather poor, the diagnostic features of the marker species are distinguishable.

#### 4.1.1. *Paragloborotalia siakensis* and *Paragloborotalia mayeri*

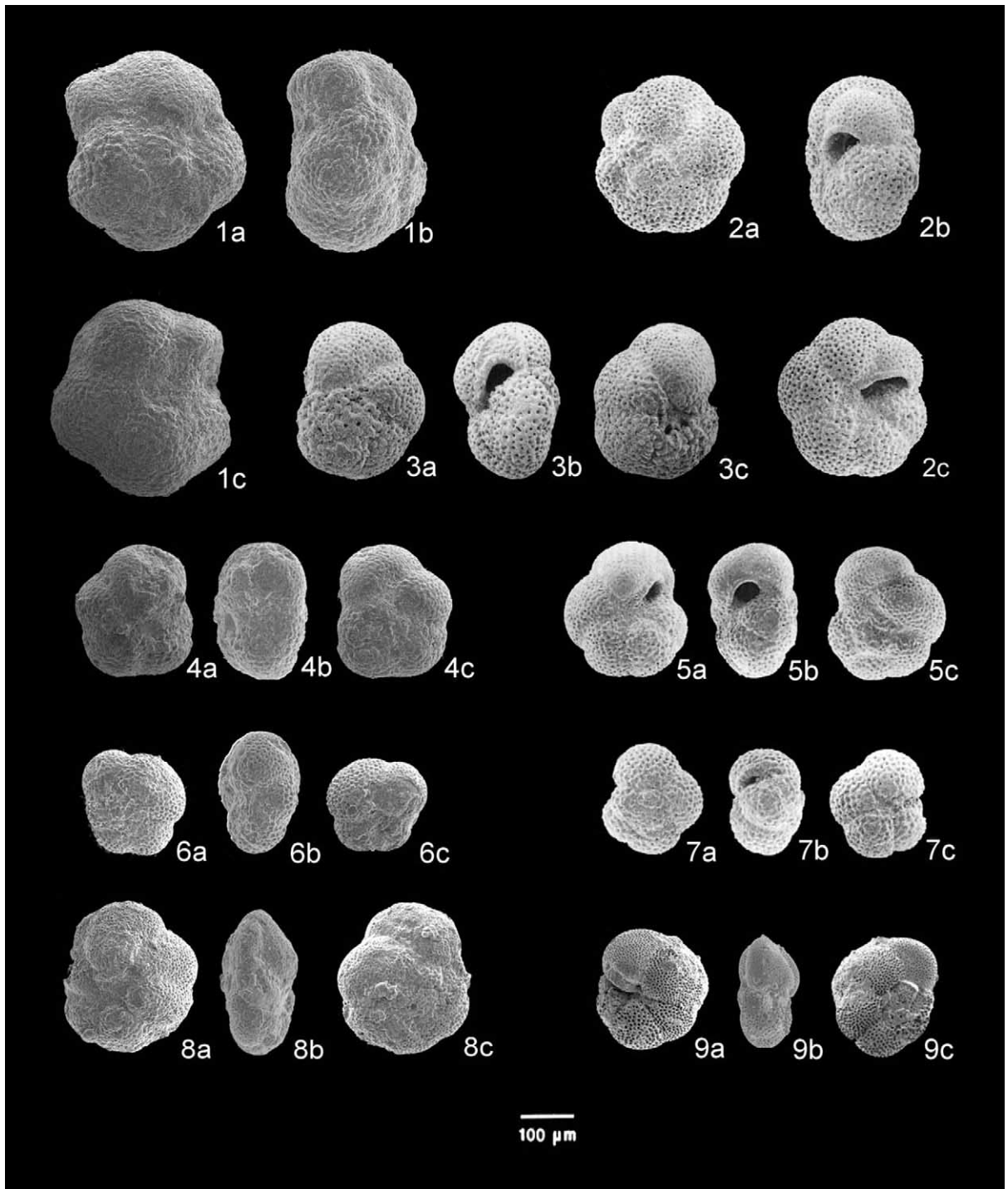
In our previous study of the Monte Gibliscemi section (Hilgen et al., 2000a) we considered *P. siakensis* as a junior synonym of *P. mayeri* following the taxonomic concept of Bolli and Saunders (1985). Other authors (e.g. Kennett and Srinivasan, 1983; Iaccarino, 1985; Foresi et al., 1998), however, follow the species concept of Blow (1969), who regarded *P. siakensis* and *P. mayeri* as distinct species. All these authors have a different opinion about the distribution range and phylogeny of *P. mayeri*. Blow (1969) and Kennett and Srinivasan (1983) reported a stratigraphic distribution of *P. mayeri* ranging from N9 to N13 and N4 to N14, evolving from either *Globorotalia peripheroronda* or *P. siakensis*, respectively. In the Mediterranean, *P. mayeri* was recorded in a short interval within the distribution range of *Globorotalia partimlabiata* (N13) in the middle Serravallian (e.g. Foresi et al., 1998, 2001, 2002a,b). Foresi et al. (2001) suggest a possible evolution of this species from *G. partimlabiata*. All this indicates that the controversy is still open and further studies are necessary to better understand taxonomy, phylogeny and stratigraphic distribution of *P. mayeri* sensu Blow (1969).

At Monte dei Corvi, we observed forms referable to *P. mayeri* with a distribution range similar to that found on Malta and Tremiti Islands (Foresi et al., 2001, 2002a,b; see Plate I, fig. 3). We kept the two species distinct in order to compare our data with those of other Mediterranean sections. However, the scarcity and poor preservation of the specimens referable to *P. mayeri* do not offer new evidence which might contribute to solve the taxonomic and biostratigraphic problems.

*P. siakensis* is a long ranging species but its distribution pattern reveals marked changes of biostratigraphic significance. *P. siakensis* is absent in the lowermost part of the section but is abundant and almost continuously present in two intervals higher in the succession between 5.58 m (Acme I Bottom) and 33.16 m (Acme I Top) and between 40.48 m (Acme II Bottom) and 52.70 m (Acme II Top). These two peak intervals have recently been found in other Mediterranean sections by Foresi et al. (2002a,b). The top of the second interval corresponds to the abundance drop of *P. mayeri* sensu Bolli and Saunders (1985) (= *P. siakensis* in this work) recorded in cycle –87 at Monte Gibliscemi and dated at 12.006 Ma (Hilgen et al., 2000a). The correlation is confirmed by the *G. partimlabiata* increase and the *Globoturborotalita apertura*–*Globigerinoides obliquus* gr. peak, which immediately follow the *P. siakensis* drop both in the Monte dei Corvi and Monte Gibliscemi sections, as well as on Tremiti Islands (Foresi et al., 2002a).

The last occurrence (LO) of *P. siakensis* at Monte dei Corvi is not a clear-cut event as at Monte Gibliscemi. Typical specimens of *P. siakensis* disappear at 72.23 m where we placed the LO of the species. The *P. siakensis* LO as defined above in the Monte dei Corvi section is found in the same relative position as at Monte Gibliscemi. Atypical and poorly preserved specimens of the species, which are discontinuously present up to 80 m, are possibly reworked.

*P. mayeri* sensu Blow (1969) is found as trace element over a short stratigraphic interval. Following a single occurrence at 28.69 m, the species is almost continuously present from 38.64 m up to 43.59 m. The LO of a single and atypical specimen is found at 51.35 m. The first and last occurrences of *P. mayeri* cannot be considered reliable events since they are based on scattered occurrences and poorly preserved specimens. Despite the scarcity of the species, however, the *P. mayeri* distribution range between 38.64 m and 51.35 m is in agreement with that observed on Malta and Tremiti Islands (Foresi et al., 2002a,b) if compared with the distribution ranges of *P. siakensis* and *G. partimlabiata*.



#### 4.1.2. Globorotalia partimlabiata

The first occurrence (FO) of *G. partimlabiata* is recorded at 28.69 m and the position of this bio-event is well comparable with that reported by Montanari et al. (1997b) at about 22 m above the Respighi Level. The taxon shows a sharp decrease in abundance at 59.55 m, about 2 m below the Ancona ash. Montanari et al. (1997b) placed their *G. partimlabiata* LO at a comparable position just below the ash. Foresi et al. (2002a) observed the same sharp decrease in abundance of *G. partimlabiata* at Tremiti Islands; according to their taxonomic concept, this level represents the actual LO of the species although they find less typical representatives at higher levels which they labelled *G. cf. partimlabiata*. According to Foresi et al. (2001) these atypical forms could be referable to *G. challengerii*. In our opinion these younger specimens, even if smaller in size, can be included in the morphological variation of *G. partimlabiata*. At Monte dei Corvi, *G. partimlabiata* vanishes higher up in the section, at 90.84 m, and its distribution pattern compares well with that observed at Monte Gibliscemi.

#### 4.1.3. Globigerinoides subquadratus

*G. subquadratus* occurs very rarely and is scattered in the lower part of the section but becomes

more abundant from about 57 m up to 63.56 m. At this level the last common occurrence (LCO) of the species is placed resulting in a slightly lower position (about two cycles) than at Monte Gibliscemi. In the Monte dei Corvi section the actual position of this event may be obscured by the presence of very poorly preserved samples and even a barren sample directly above this level. The distribution pattern of *G. subquadratus* compares well with that recorded on Tremiti Islands (Foresi et al., 2002a) and in the Case Pelacani section on Sicily (di Stefano et al., 2002).

#### 4.1.4. Globoturborotalita apertura– Globigerinoides obliquus group

We lumped *G. apertura*, *G. decoraperta* and *G. obliquus* under this label to maintain a stable taxonomic concept even under poor preservation conditions and to compare the distribution pattern of this taxon with that observed at Monte Gibliscemi (Turco et al., 2001). This group, which occurs very rare and scattered in the lower part of the section, becomes more continuous and abundant from about 51 m upwards. Following a major influx located just above the top of the second peak interval of *P. siakensis*, it becomes truly abundant and continuously present from 65.18 m up to the top of the section. The first regular

---

#### Plate I.

1. *Paragloborotalia siakensis* (LeRoy): 1a spiral view, 1b axial view, and 1c umbilical view; Monte dei Corvi section, sample It 20383, 8.13 m.
2. *Paragloborotalia siakensis* (= *P. mayeri* in Hilgen et al., 2000a): 2a spiral view, 2b axial view, and 2c umbilical view; Monte Gibliscemi section, sample It 18516.
3. *Paragloborotalia mayeri* (Cushman and Ellisor) sensu Blow (1969): 3a spiral view, 3b axial view, and 3c umbilical view; Tremiti Islands, sample TTA-86 (after Foresi et al., 2002a).
4. *Globorotalia partimlabiata* Ruggieri and Sprovieri: 4a umbilical view, 4b axial view, and 4c spiral view; Monte dei Corvi section, sample It 20413, 28.69 m.
5. *Globorotalia partimlabiata* Ruggieri and Sprovieri: 5a umbilical view, 5b axial view, and 5c spiral view; Monte Gibliscemi section, sample It 18553.
6. *Neogloboquadrina acostaensis* s.s. (Blow): 6a spiral view, 6b axial view, and 6c umbilical view; Monte dei Corvi section, sample It 20530, 62.28 m.
7. *Neogloboquadrina acostaensis* s.s. (Blow): 7a spiral view, 7b axial view, and 7c umbilical view; Monte Gibliscemi section, sample It 18575.
8. *Globorotalia peripheroronda* Blow and Banner: 8a umbilical view, 8b axial view, and 8c spiral view; Monte dei Corvi section, sample It 20397, 17.95 m.
9. *Globorotalia peripheroronda* Blow and Banner: 9a umbilical view, 9b axial view, and 9c spiral view; Tremiti Islands, sample It 19597.

occurrence (FRO) of the group is placed at this level, which is in the same relative position as in section GIBLISCEMI.

Our *G. apertura*–*G. obliquus* gr. FRO corresponds to the FRO of *G. obliquus obliquus* recorded on Tremiti Islands (Foresi et al., 2002a) and in the Case Pelacani section (di Stefano et al., 2002), and is considered to be a very useful event in the Mediterranean area (e.g. Foresi et al., 1998; Sprovieri et al., 2002a,b). In addition, the *G. apertura*–*G. obliquus* gr. FRO marks a significant change in species composition of the oligotrophic tropical-subtropical planktonic foraminiferal assemblage related to the global cooling associated with the Mi-5 oxygen isotope event (Turco et al., 2001).

#### 4.1.5. *Globorotaloides falconarae*/Catapsydrax parvulus

*G. falconarae* was first described by Giannelli and Salvatorini (1976) from the Mediterranean area. Small-sized specimens of *G. falconarae* are virtually indistinguishable from *C. parvulus*, described by Bolli (1957) from Trinidad. For this reason, Zachariasse (1992) and Hilgen et al. (1995) considered *G. falconarae* as a junior synonym of *C. parvulus*. Later on, Hilgen et al. (2000a) suggested that *G. falconarae* and *C. parvulus* are homeomorphs and phylogenetically unrelated. In fact, *G. falconarae* seemed to have evolved from *Globoquadrina* sp.1 around 11.5 Ma, whereas the range of the low-latitude *C. parvulus* extends back into the early Miocene. Recently, Foresi et al. (2001) embraced again the idea of synonymy between *G. falconarae* and *C. parvulus* based on their morphological resemblance and suggested that the *C. parvulus* holotype as figured by Bolli (1957) is actually a juvenile form, which apparently differs from the *G. falconarae* holotype in wall texture.

In the Mediterranean area, similar forms, labelled either *G. falconarae* or *C. parvulus*, have been found in sections of Langhian (Fornaciari et al., 1997; Foresi et al., 2001) and late Serravallian to Tortonian age (Hilgen et al., 1995, 2000a; Foresi et al., 2002a). The same distribution is also observed at Equatorial Atlantic Site 926 (Turco et al., 2002) and at North Atlantic Site 397 (Foresi

et al., 1998, 2001). Apparently, these forms are absent in the Mediterranean and low-latitude Atlantic Ocean during the early Serravallian.

However very rare small-sized specimens referable to *G. falconarae*/*C. parvulus* are discontinuously present in the lower Serravallian at Monte dei Corvi, in an interval older than the base of section GIBLISCEMI. The taxon becomes continuously present from 60.34 m upward and is more abundant from 79.48 m up to the top of the section. The rare occurrence of the taxon in the lower Serravallian calls our previous suggestions about the origin of *G. falconarae* and the homeomorphism between *G. falconarae* and *C. parvulus* into question. In fact, we may better reconsider them as *C. parvulus* following the earlier concept of Zachariasse (1992) also because similar forms extend back into the Langhian. However their presence in the lower Serravallian has only been evidenced at Monte dei Corvi (this study) but not on the Tremiti Islands or Malta (Foresi et al., 2002a,b,c). Further studies are necessary to better document the exact distribution range of this taxon in order to re-evaluate the synonymy between *C. parvulus* and *G. falconarae*.

#### 4.1.6. *Neogloboquadrina* group

We maintained the same subdivision of the *Neogloboquadrina* group in four types as in our study of the GIBLISCEMI section (Hilgen et al., 2000a): large-sized *N. atlantica*, small-sized *N. atlantica*, *N. acostaensis* sensu strictu (s.s.) and the so-called four-chambered type. The latter is included in *N. acostaensis* according to our concept of the species (for more details on taxonomy, see Hilgen et al., 2000a). Recently, it has been proposed to label our large- and small-sized *N. atlantica* as *N. atlantica atlantica* and *N. atlantica praeatlantica* respectively, while the four-chambered type was lumped together with *N. acostaensis* s.s. (Foresi et al., 2002c). However, we preferred to maintain our previous taxonomic subdivision of neogloboquadrinids to better compare their distribution with Monte GIBLISCEMI.

At Monte dei Corvi, neogloboquadrinids first occur at 59.80 m directly above a drop in the abundance of *G. partimlabiata* like in section GIBLISCEMI. The neogloboquadrinids are mainly rep-

resented by small-sized *N. atlantica* and, to a lesser extent, the four-chambered type. *N. acostaensis* s.s. is very rare and first occurs at 60.34 m, i.e. at a slightly younger level with respect to the other two *Neogloboquadrina* types.

The distribution pattern of the *Neogloboquadrina* group at Monte dei Corvi is very similar to that observed at Monte Gibliscemi. They are continuously present between 59.80 and 63.84 m (first influx) but become very rare and are discontinuously present from 64.23 to 73.11 m, where the base of the second influx is placed. *Neogloboquadrinids* represent a major component of the planktonic foraminiferal assemblage from this last level up to the top of the section. However, the base of the second *neogloboquadrinid* influx coincides with the FO of large-sized *N. atlantica* at Monte dei Corvi, whereas the same event predates the large-sized *N. atlantica* FO at Monte Gibliscemi (Hilgen et al., 2000a). This discrepancy is most likely due to the very poor preservation of the samples in the interval directly below 73.11 m.

Changes in coiling direction of the *neogloboquadrinids* observed at Monte Gibliscemi are easily recognized at Monte dei Corvi confirming their biostratigraphic significance in the Mediterranean region; they are randomly coiled between 59.80 and 63.84 m and predominantly dextrally coiled between 73.11 and 89.18 m. The *neogloboquadrinids* reveal further changes in coiling direction in the uppermost part of the section, namely from dextral to sinistral at 89.82 m and from sinistral to dextral at 91.53 m.

The distribution range of large-sized *N. atlantica* and the position of the last regular occurrence (LRO) of small-sized *N. atlantica* are in good agreement with the position of the same events at Monte Gibliscemi. The large-sized *N. atlantica* FO is placed at 73.11 m and the LO at 77.81 m. The taxon is intermittently present and shows a number of abundance peaks in sapropel layers. The LRO of small-sized *N. atlantica* at 83.32 m is a distinct event and is found in the same position as in section Gibliscemi. In contrast, the FRO of *N. acostaensis*, as defined at Monte Gibliscemi, is considered a less distinct and easily recognizable event even though it has been identified at Case Pelacani (Caruso et al., 2002).

#### 4.1.7. *Globorotalia scitula* and *Globorotalia menardii* group

Beside the distribution of the main biostratigraphic markers, we analyzed the distribution pattern of the *G. scitula* and *G. menardii* groups because of their potential biostratigraphic value. The *G. scitula* group is present throughout the section except for an interval between 10.04 m and 24.30 m where it is extremely rare and discontinuously present. The presence of the *G. scitula* gr. in the lower part of the section in combination with the concomitant absence of *P. siakensis* might be a valuable biostratigraphic tool to characterize the lower Serravallian below the base of the first acme interval of *P. siakensis* down to the LRO of *G. peripheroronda*. The same pattern of the *G. scitula* gr. and *P. siakensis* has also been recorded at Tremiti Islands (unpublished data).

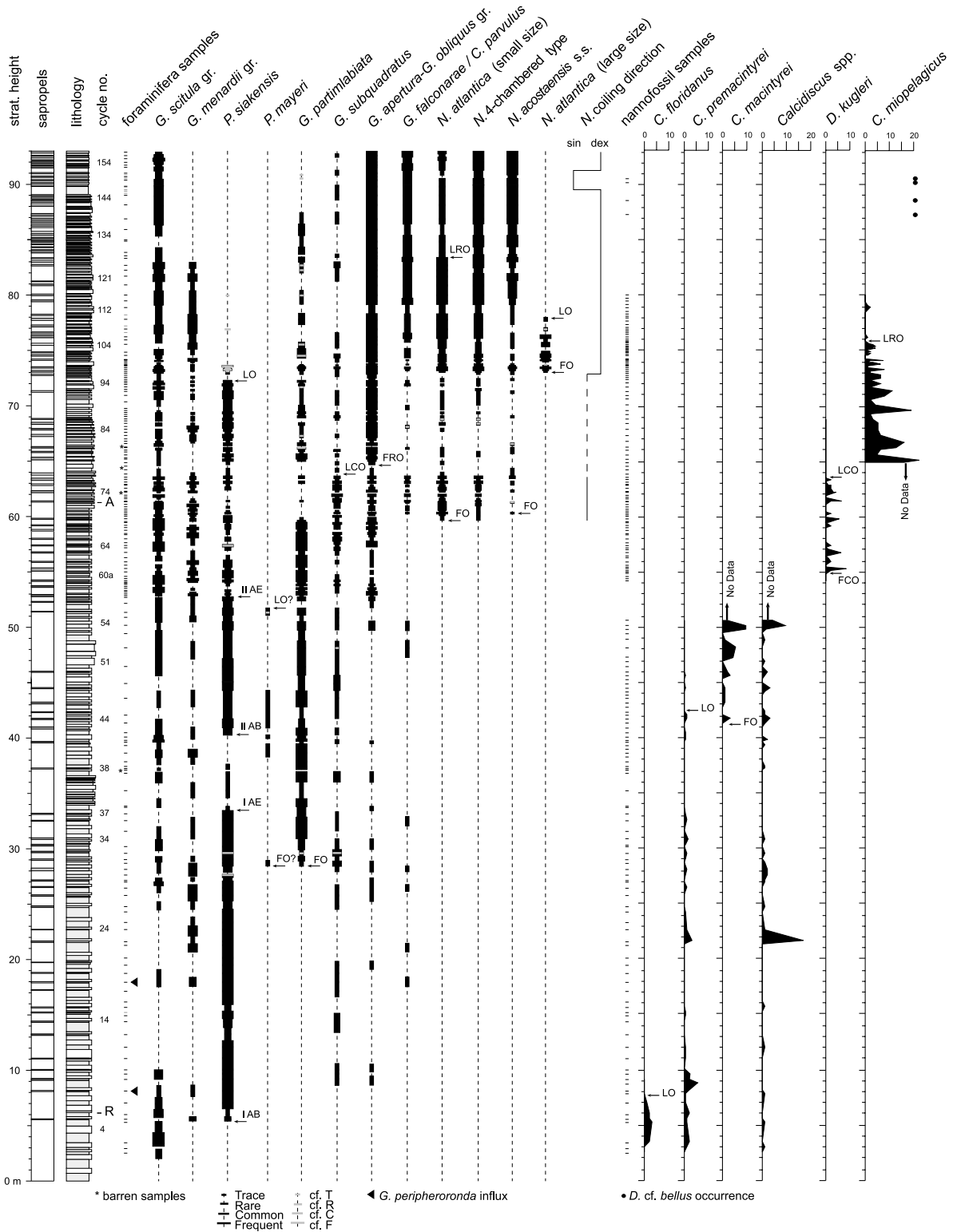
The *G. menardii* group occurs very scattered in the lowermost 20 m of the section, but becomes more abundant although discontinuously present higher up in the section. The group vanishes at about 83 m at a stratigraphic level that approximates the LRO of *N. atlantica* (small-sized), i.e. similar to the Monte Gibliscemi section (Turco et al., 2001).

#### 4.1.8. *Globorotalia peripheroronda* influxes

We observed two short influxes of *G. peripheroronda* at 8.13 m and 17.95 m in our section. These two influxes have also been recognized on Tremiti Islands in the correlative sedimentary cycles (unpublished data), thus showing their potential value for high-resolution biostratigraphic correlations in the Mediterranean. The *G. peripheroronda* LO has been recorded and dated astronomically at 13.39 Ma on Malta (Sprovieri et al., 2002a; Foresi et al., 2002b), i.e. at a level older than the base of our Monte dei Corvi section. Both our influxes occur in the first acme interval of *P. siakensis*, while the *G. peripheroronda* LO of Foresi et al. (2002b) is found well below this interval.

#### 4.2. *Calcareous nannofossils*

Calcareous nannofossil assemblages of Monte



dei Corvi were previously analyzed by Fornaciari et al. (1996) in a biostratigraphic study of the Mediterranean Middle Miocene. Through a quantitative analysis of the same samples studied in detail by Coccioni et al. (1992) and Montanari et al. (1997b), they recognized the following biohorizons in the Serravallian to lower Tortonian part of the section, listed from older to younger as follows: *Calcidiscus premacintyreus* last common occurrence (LCO); *Calcidiscus macintyreus* first occurrence (FO); *Coccolithus miopelagicus* LCO; *Helicosphaera walbersdorfensis* last occurrence (LO); *Helicosphaera stalis* first common occurrence (FCO); *Discoaster bellus* group FO, and; *Discoaster hamatus* FO.

In this study we analyzed the nannofossil assemblages in selected intervals of the section with the purpose to refine the previous biostratigraphy, and examine additional biohorizons such as the *Discoaster kugleri* FCO and LCO and the *Cyclicargolithus floridanus* LO. Analyses focused mainly on the lower part of the section and on intervals that overlap stratigraphically with the Gibli-scemi section.

Quantitative data were collected on selected samples using standard techniques for smear slide preparation and a polarizing light microscope. Abundances of the index species were obtained by counting the number of specimens of each index species per unit area of the slide. The distribution patterns of the selected marker species (Fig. 5) allow to locate the position of the biostratigraphic useful events.

Identification of the nannofossils was often obscured by the strong overgrowth that affected the assemblages especially in samples from the marls and marly limestones. This generally poor preservation prevented us from obtaining reliable data on some index species. In addition, it was not possible to obtain reliable data on the distribution of small helicoliths like *H. stalis* and *H. walbersdorfensis*, whose specimens were only sporadically

encountered. Discoasterids are present throughout the studied interval but are generally rare and poorly preserved. Identification of *Discoaster* species was possible only in samples from the sapropel layers. Placoliths belonging to the *Coccolithus* and *Calcidiscus* genera are present as minor secondary components in the assemblages whereas *Reticulofenestra* and *Dictyococcites* prevail: peaks in abundance of small specimens of the latter two genera were observed in some intervals within the marly limestones.

Results of the biostratigraphic analysis and the biohorizons identified are reported below and discussed in comparison with previous data from Monte dei Corvi (by Fornaciari et al., 1996) and with biostratigraphic data from the Monte Gibli-scemi, Case Pelacani, Tremiti Island and Ras il-Pellegrin sections (Hilgen et al., 2000a; Caruso et al., 2002; Foresi et al., 2002a,b) and the open ocean.

#### 4.2.1. *Cyclicargolithus floridanus* LO

We observed very rare specimens of *C. floridanus* in the basal part of the section just below the Respighi ash layer. It is difficult to ascertain whether their presence is due to reworking or represents the uppermost part of the *C. floridanus* distribution range. Nevertheless, the presence of specimens of *Reticulofenestra pseudoumbilicus* in the same interval and its gradual upward increase in abundance suggest that the basal part of the section is very close to the *C. floridanus* LO. This is in agreement with data from open ocean sites, in which the decrease (LCO) and extinction (LO) of *C. floridanus* are linked to the appearance (FO) and increase (FCO) of *R. pseudoumbilicus*. Although the exit of *C. floridanus* and entrance *R. pseudoumbilicus* are recorded at different stratigraphic levels in different oceanic areas (see Raffi et al., 1995), their distribution ranges are invariably associated (*R. pseudoumbilicus* increases just above the sharp decrease in *C. floridanus*).

Fig. 5. Semi-quantitative distribution patterns of planktonic foraminiferal marker species and quantitative distribution patterns of calcareous nannofossil marker species against depth in the Monte dei Corvi section. No data indicates that the species has not been counted in that particular interval.

Relative to the base of the first acme interval of *P. siakensis*, the observed specimens of *C. floridanus* are found at a higher stratigraphic level than the *C. floridanus* LCO recorded in the Ras il-Pellegrin section on Malta (Foresi et al., 2002b), indicating that they are similar to the sporadic specimens often encountered above the LCO horizon (Fornaciari et al., 1996).

#### 4.2.2. *Calcidiscus macintyre* FO, and *Calcidiscus premacintyre* LO and LCO

The usefulness of the *C. macintyre* FO, and the *C. premacintyre* LO and LCO for biostratigraphic subdivision of the Mediterranean Miocene was investigated and discussed in detail by Fornaciari et al. (1996). These authors used the *C. premacintyre* LCO to define their MNN6/7 zonal boundary and showed that it is concomitant with or occurs just above the *C. macintyre* FO, as in records from the open ocean (see discussion in Fornaciari et al., 1996). Both biohorizons are not clear-cut, and the weakness of the signals becomes particularly evident if nannofossil assemblages are poorly preserved, thus complicating biostratigraphic observations. Moreover, the *C. macintyre* distribution is known to be biogeographically controlled (Raffi et al., 1995), which in addition affects the degree of reliability of biohorizons associated with the species.

The previous study of the Monte dei Corvi section by Fornaciari et al. (1996) documented the distribution of both index species. The extinction pattern of *C. premacintyre*, the appearance pattern of *C. macintyre* and the position of both biohorizons relative to each other agree well with data available from the Mediterranean and the open ocean (Raffi et al., 1995). In the present study we analyzed the *Calcidiscus* index species in all samples available from the lowermost 51 m in our section. *Calcidiscus* specimens are generally rare and completely missing in many samples resulting in an intermittent distribution pattern (Fig. 5). As a consequence, the biostratigraphic signal is weak for both index species, but the two biohorizons nevertheless maintain their reciprocal positions, with the *C. macintyre* FO recorded at 41.72 and the *C. premacintyre* L(C)O at 42.07 m. These data agree with the results of

Fornaciari et al. (1996), who recognized the two biohorizons in the interval 11 to 14 m below the Ancona ash layer.

Relative to the base of the second *P. siakensis* acme interval, our *C. macintyre* FO and *C. premacintyre* L(C)O correspond rather well with the *C. macintyre* FCO and *C. premacintyre* LO reported by Foresi et al. (2002a) from Tremiti Islands. However they occur at a much higher level than the *C. macintyre* FO and *C. premacintyre* LCO reported from Tremiti Islands and Malta; the latter events are located just above the *G. partimlabiata* FO (Foresi et al., 2002a,b). These differences at least partly reflect the difficulties encountered in accurately defining and pinpointing these events in the Mediterranean due to the weakness of the biostratigraphic signal.

#### 4.2.3. *Discoaster kugleri* FCO and LCO

The presence of *D. kugleri* passed unobserved in the previous study of the Monte dei Corvi section because the species was known to be very rare and therefore not considered useful for biostratigraphic purposes in the Mediterranean Miocene (Fornaciari et al., 1996). Moreover discoasterids are rare and poorly preserved at Monte dei Corvi. The usefulness of the *D. kugleri* biohorizons for biostratigraphic subdivision of the Mediterranean Miocene was first demonstrated by Hilgen et al. (2000a). In their study of section Gibliscemi, they recorded a short interval in which *D. kugleri* is continuously present often in elevated numbers. The astronomical ages for the *D. kugleri* FCO and LCO at Gibliscemi are consistent with the astronomical ages obtained for the same events in the low-latitude open ocean, where the species is common in a short interval and the two biohorizons are clearly documented (Raffi et al., 1995; Backman and Raffi, 1997). In the light of these findings, a detailed analysis was carried out at Monte dei Corvi with the purpose to detect the *D. kugleri* range in this section. Our investigation concentrated on samples from the sapropel layers, in which the preservation of discoasterids is considerably better than in samples from the marly limestone beds. We obtained a clear picture of the distribution pattern of *D. kugleri* (see Fig. 5), despite the poor preservation of

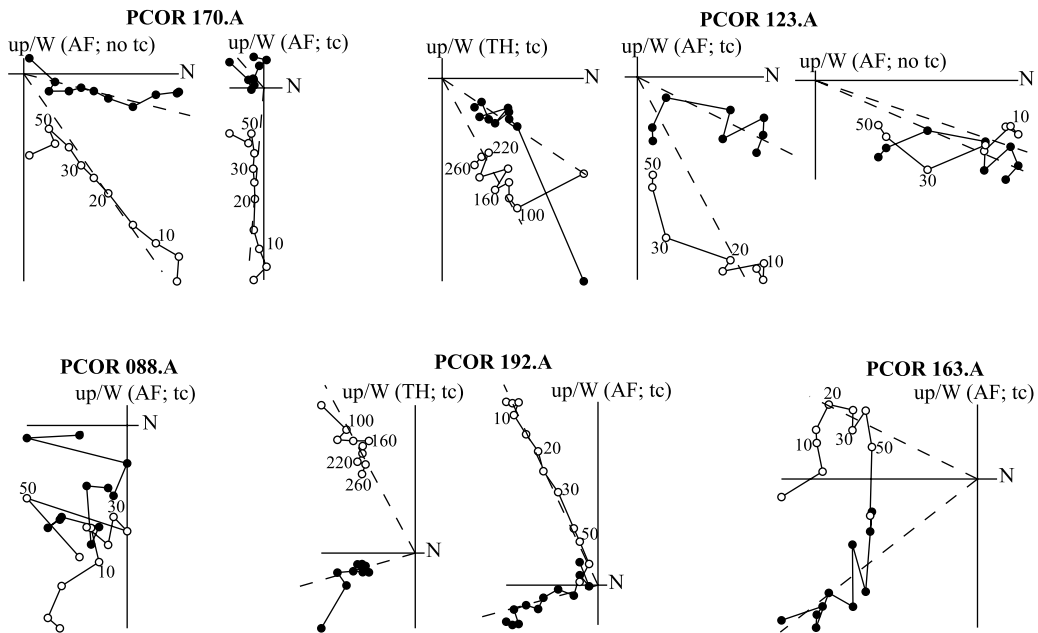


Fig. 6. Representative examples of thermal (TH) and alternating field (AF) demagnetization diagrams. Closed (open) symbols represent the projection of vector end-points on the horizontal (vertical) plane; values denote temperature in degrees Celsius (°C). (No) tc indicates that (no) tectonic correction for the bedding tilt has been made.

the specimens and the fact that the species is present in low numbers only. The short interval in which the species is found extends from 55.31 to 63.36 m, where the FCO and LCO biohorizons are placed, respectively.

The position of these events corresponds well with the positions of the same events reported from the Gibliscemi, Case Pelacani and Tremiti Island sections (Hilgen et al., 2000a,b,c; Foresi et al., 2002a; Caruso et al., 2002).

#### 4.2.4. *Coccolithus miopelagicus* LRO

The position and pattern of the LRO of *C. miopelagicus* is similar to that observed at Monte Gibliscemi and is consistent with the foraminiferal data. The biohorizon is close to the *P. mayeri* LO (it occurs just above it, at 75.55 m). The species is scarce and irregularly distributed in the upper part of its range and marked by decreases in abundance (it disappears for short intervals) just below the LRO biohorizon. Our analysis resulted in a more detailed picture of the distribution of *C. miopelagicus* than reported by Montanari et al. (1997b), who placed the LCO of *C. miopelagicus*

(equivalent to our LRO) at a somewhat lower stratigraphic position, about 10 m above the Ancona ash layer. Relative to the foraminiferal data, the *C. miopelagicus* LCO is also reported from a lower stratigraphic level in the Case Pelacani section (Caruso et al., 2002).

#### 4.2.5. *Helicosphaera stalis* FCO and *Helicosphaera walbersdorfensis* LO

The determination of the distribution patterns of these two species of small helicoliths in their uppermost (for *H. walbersdorfensis*) and lowermost (for *H. stalis*) ranges was hampered by preservation problems and differences in the composition of the nannofossil assemblages. At Monte dei Corvi, the biostratigraphic signal is unclear mainly due to the discontinuous presence of the index species rather than to the poor preservation of the assemblage. Scattered presences of *H. walbersdorfensis* and *H. stalis* were recorded at different levels within the studied interval, i.e. below 77 m and above 85 m, respectively. We failed to detect the two successive events (or the reversal in abundance between the two species) in our high

resolution sample set, despite the fact that they have previously been recorded in the same section (Fornaciari et al., 1996) and elsewhere in the Mediterranean (Fornaciari et al., 1996; Hilgen et al., 2000a). The distribution of these small helicoliths seems to be controlled by environmental factors even over a limited geographic area (within the Mediterranean). Similar discrepancies in the distribution of small helicoliths have been observed between sedimentary successions from the late Miocene in the Mediterranean (Raffi, unpublished data).

#### 4.2.6. *Discoaster hamatus* FO and *Discoaster bellus* group FO

The appearance of the five-rayed discoasterids (*D. bellus* gr. FO) in the Mediterranean has been considered a fairly reliable event (Fornaciari et al., 1996). It is succeeded by the *D. hamatus* FO, an event which is usually difficult to pinpoint due to the rareness of the marker species. Despite the inferred reliability of the *D. bellus* gr. FO, we failed to recognize this biohorizon at Monte dei Corvi. Single specimens of *Discoaster* cf. *bellus* were recorded in some samples (at 87.24, 88.48, 90.09, and 90.37 m). These scattered presences are found in the same position as the oldest five-rayed discoasterids at Monte Gibliscemi (Hilgen et al., 2000a).

### 5. Magnetostratigraphy

The Monte dei Corvi section has previously been subjected to a detailed paleomagnetic study by Montanari et al. (1997b). Applying standard demagnetization techniques, they concluded that the magnetic intensity was too weak to yield useful information on the magnetic polarity and that the natural remanent magnetization (NRM) was already largely removed at a temperature of 200°C. Nevertheless, several samples showed southwesterly declinations and negative inclinations, but these directions were considered as an overprint. Furthermore, rock magnetic experiments revealed that there was no significant difference in magnetic mineralogy or grain size throughout the section (Montanari et al., 1997b).

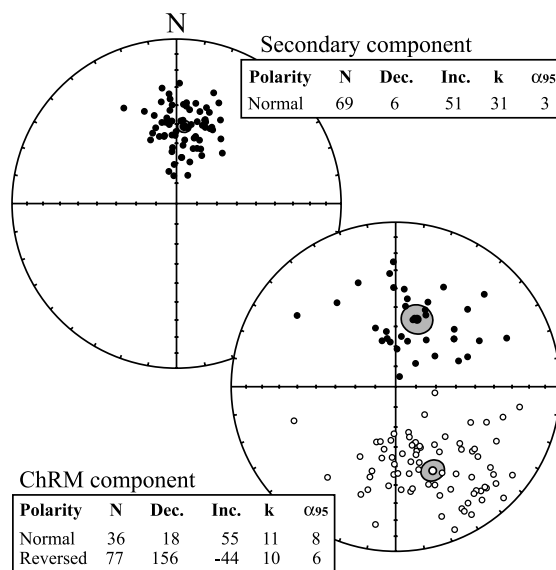


Fig. 7. Plotted directions of the secondary and ChRM component showing the non-antipodality of the latter. The 95% confidence ellipse for the normal and reverse mean directions is indicated. Statistical information: N, number of samples; Dec., declination; Inc., inclination; k, Fisher's precision parameter,  $\alpha_{95}$ , radius of the 95% confidence cone.

A pilot study on a limited number of oriented hand samples similarly revealed weak to very weak NRM intensities, but also some levels with opposite reversed and normal polarity directions. In view of its manifest importance we resampled Monte dei Corvi with an approximate resolution of one sample per cycle (that is 20 kyr) despite these rather discouraging results. All 192 samples were taken with a portable drill and a generator as power supply. Evidently, the 40° tilt (bedding orientation 110/42; strike/dip) will help to distinguish primary (pre-tilt) from secondary (post-tilt) components.

Stepwise alternating field (AF) demagnetization was applied to at least one specimen per level. Small steps of 5 mT were applied up to 30 mT, followed by steps of 10 mT up to a maximum field of 100 mT. In addition, thermal (TH) demagnetization was applied to the second specimen (when available) with temperature increments of 20°C after an initial heating step to 100°C. Samples were heated and cooled in a laboratory-built, shielded furnace with a residual field of less than

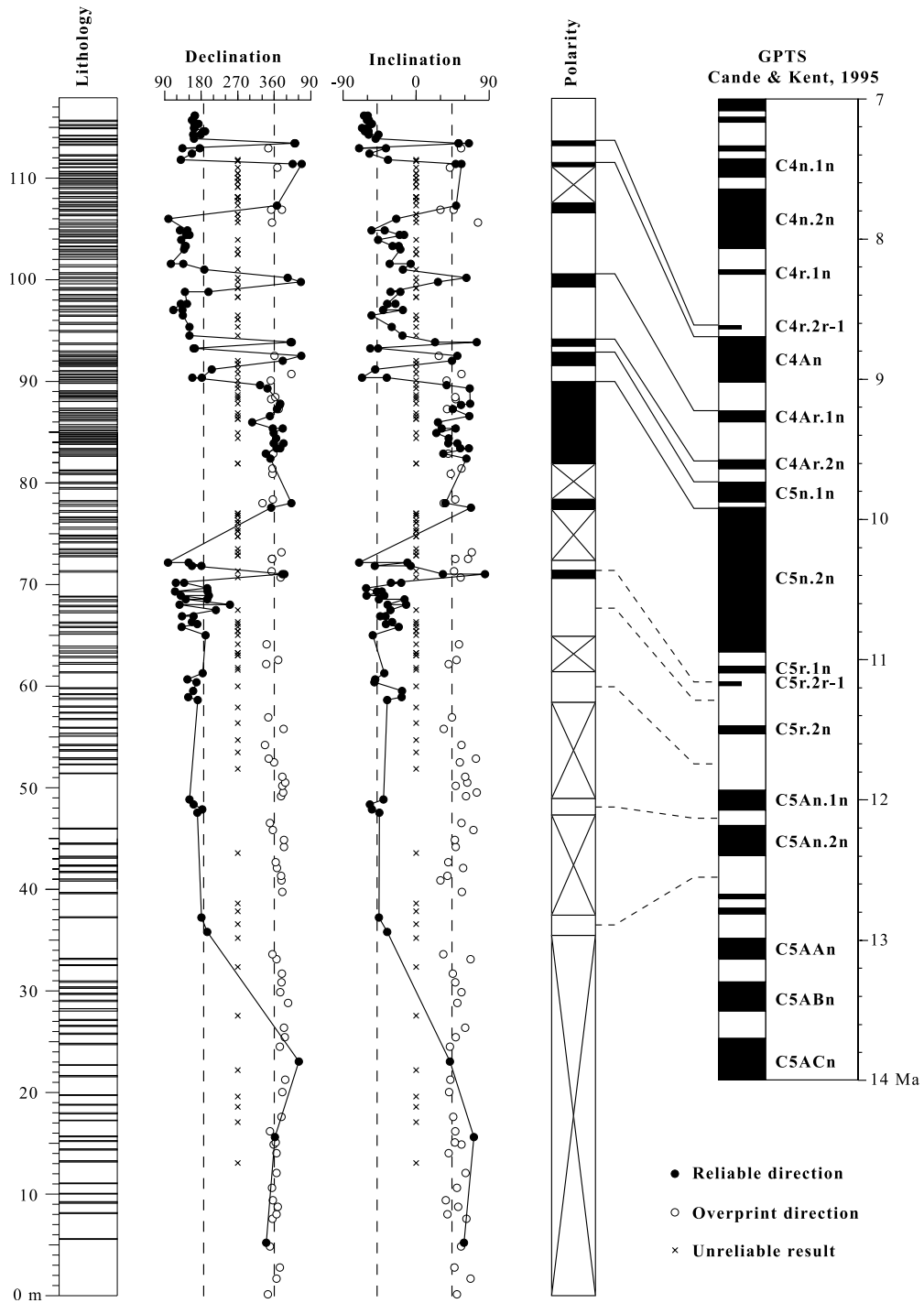


Fig. 8. Magnetostratigraphy of Monte dei Corvi and correlation to CK95. In the polarity column black (white) denotes normal (reversed) polarity intervals and cross-hatching denotes intervals of undefined polarity.

30 nT. The NRM was measured at each step with a horizontal 2G Enterprises DC SQUID cryogenic magnetometer. NRM directions were determined by means of principal component analysis and magnetization vectors were averaged using Fisher statistics to calculate the mean direction per component.

The initial NRM invariably revealed very weak intensities ranging between 0.05 and 0.6 mA/m. It proved impossible to determine the magnetic components from Zijderveld diagrams in a significant number of samples ( $\pm 25\%$ ); directions showed so much scatter that it was not even possible to determine their polarity (Fig. 6; PCOR 088). Most samples from the lower half of the section — but several levels from the upper half as well — revealed a normal polarity component in geographic coordinates (Fig. 6; PCOR 170) but the orientation of this component often changed into meaningless directions following tectonic correction (tc) for the bedding tilt. We interpret this component as a secondary post-tilt overprint probably related to the present-day field. Although directions show some scatter in all samples, the average direction of this secondary component approximately coincides with the expected direction at the location (43°N; inclination of 62° see also Fig. 7).

In contrast, samples from the uppermost part of the section revealed a straightforward reversed component that decays linearly towards the origin in fields between 10 and 60 mT and temperatures between 100 and 260°C (Fig. 6; PCOR 192). Directions were obtained following tectonic correction, indicating that the component is pre-tilt, and therefore most likely of primary origin. In addition, no evidence is found at all of a secondary overprint. Other levels revealed a reversed component in the same field/temperature range, but an additional secondary normal overprint is present (Fig. 6; PCOR 163). This secondary component could be largely removed at very low fields (0–10 mT) and temperatures (0–120°C). Demagnetizations showing normal pre-tilt directions are observed in the upper part of the section, especially in the interval between 75 and 95 m. (Fig. 6; PCOR 123), although their quality is less as in the reversed uppermost part. Isolated normal

components mainly show north to northeast declinations and a rather disorderly decay towards the origin, thereby hampering a reliable determination of the direction.

Summarizing, sediments from section Monte dei Corvi revealed a complex NRM behavior with two partly overlapping components. It proved possible to isolate a characteristic component marked by dual polarities. This characteristic remanent magnetization (ChRM) component shows two clusters located in the SE and NE quarters of an equal area plot (Fig. 7). The non-antipodal behavior can be explained by overlapping unblocking temperature spectra of a primary component and the secondary (post-tilt) overprint making it impossible to completely isolate the primary ChRM component. We thus assume that this component records the ancient geomagnetic field, even though it does not pass the reversal test. Mean directions of the ChRM should therefore be treated with caution when interpreted in terms of tectonic rotations.

Plotting the ChRM directions in stratigraphic order reveals three isolated intervals of reversed polarity in the lowermost 60 m of the section, which is dominated by secondary components (Fig. 8). By contrast, 14 polarity reversals are recorded in the uppermost 60 m, which reveal a prolonged interval of normal polarity between 75 and 90 m (Fig. 8). This interval has a minimum duration of 700 kyr if the small-scale cycles are related to precession. Accepting a precession origin for the sedimentary cyclicity, we can correlate the normal polarity interval with chron C5n.2n, because it is the only normal chron in this part of the geomagnetic polarity time scale (GPTS) with a duration in excess of 700 kyr (Cande and Kent, 1995). The three small normal subchrons between 90 and 100 m then correspond to C5n.1n, C4Ar.2n and C4Ar.1n and the uppermost normal polarity interval at 114 m to cryptochron C4r.2r-1 (Fig. 8). Unfortunately, all these normal polarity intervals are marked by one or two samples only. This indicates that some caution is required here even though the correlative subchrons in the GPTS (CK95: Cande and Kent, 1995) show relatively short durations varying between 40 and 100 kyr.

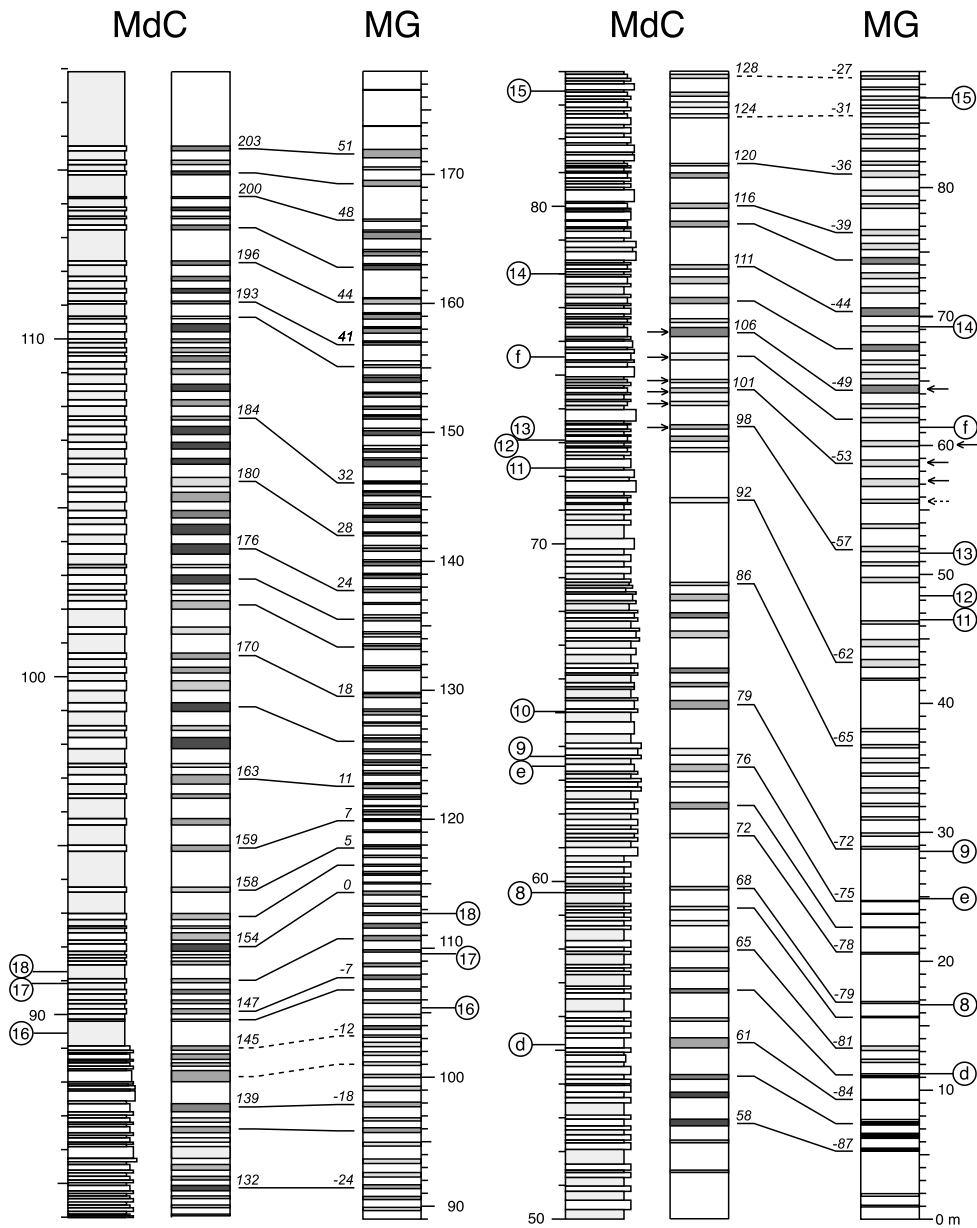


Fig. 9. Cyclostratigraphic and (calcareous plankton) biostratigraphic correlations between the – upper part of the – Monte dei Corvi section and section Gibliscemi. Numbered calcareous plankton events refer to the numbers for the same events in [Table 2](#).

In conclusion, the magnetostratigraphic calibration of the upper part of section Monte dei Corvi to CK95 seems rather straightforward. However, significant discrepancies occur in the relative length of the subsequent polarity intervals. In particular the reversed intervals at 90–92 and 101–

107 m are too long when compared to the pattern in the GPTS. But our cyclostratigraphic interpretation does not point to higher sedimentation rates in these intervals. The two most logical explanations for the observed discrepancies therefore are: (1) errors in the CK95 pattern due to

changes in seafloor spreading rates and/or difficulties in determining the boundary of short sub-chrons in seafloor anomaly profiles, and (2) errors in determining the exact position of the reversal boundaries in section Monte dei Corvi. In view of the relatively low sample resolution and the poor quality of many of the demagnetizations, we presently favor the second option. Whatever its origin a much higher sample resolution with at least five levels per cycle is necessary to solve the observed discrepancies.

## 6. Astronomical tuning

### 6.1. Correlation to section Giblecemi and astronomical origin of the cyclicity

Biostratigraphic correlations between Monte dei Corvi and the Giblecemi section located on Sicily are straightforward. The calcareous plankton biostratigraphy of Monte dei Corvi reveals the same order of events as in section Giblecemi (Figs. 5 and 9). Biostratigraphic tie points were employed as a starting point to correlate the sections cyclostratigraphically in detail. The cyclostratigraphic correlations are generally straightforward because the cycle patterns are identical or nearly identical. Minor discrepancies are most likely related to the locally intense deformation in section Giblecemi which prevented us from logging the entire succession in a perfectly reliable way. Our correlations show that most of the bio-events are recorded in the correlative cycle in both sections (Fig. 9). The cyclostratigraphic correlations in addition reveal that the normal polarity intervals at 94 and 100 m correlate with two normal polarity intervals in section Giblecemi A previously identified as C4Ar.1n and C4Ar.2n while the normal polarity interval at 113 m correlates with the short normal polarity interval in section Metochia previously identified as C4r.2r-1 (Krijgsman et al., 1995). Clearly these correlations confirm both the primary character of the inferred ChRM component and the magnetostratigraphic calibration to CK95.

In principle, cyclostratigraphic correlations could have been established independently from

the biostratigraphic and magnetostratigraphic data by using characteristic details in the cycle patterns alone. This is especially true for the top part of the section, i.e. the interval from cycle 146 to 203 (Fig. 9). The similarity in the cycle patterns cannot be explained other than that the brownish organic-rich layers at Monte dei Corvi correspond to sapropels – and associated gray marlbeds – at Monte Giblecemi. This relationship is confirmed by rare influxes of large-sized *Neogloboquadrina atlantica* which are recorded in a limited number of (successive) sapropels at Monte Giblecemi and in the correlative brownish layers at Monte dei Corvi. It is for these reasons that we adopted the term sapropel instead of black shales for the brownish layers at Monte dei Corvi.

The correlations between Monte dei Corvi and Monte Giblecemi confirm the astronomical control on the sedimentary cyclicity. Further confirmation comes from the  $^{40}\text{Ar}/^{39}\text{Ar}$  dating of biotites from the Respighi and Ancona ash layers, dated at 12.86 and 11.43 Ma, respectively (Montanari et al., 1997b). Application of these ages results in an average period of close to 20 kyr for basic cycles in the interval between the ash layers and, hence, of  $\sim 40$  kyr for the intermediate cycle and of  $\sim 100$  and  $\sim 400$  kyr for the larger-scale cycles. This outcome is consistent with results of spectral analysis on a high-resolution carbonate record which point to a similar orbital control if the  $^{40}\text{Ar}/^{39}\text{Ar}$  ages of the ash layers are taken as age calibration points to compute the carbonate time series (Cleaveland et al., 2002).

### 6.2. Astronomical tuning

Now that the astronomical origin of the sedimentary cyclicity at Monte dei Corvi has been well substantiated, determination of phase relations between sedimentary cycles and individual astronomical parameters is a logical next step in an astronomical tuning procedure. For Monte dei Corvi, these phase relations can be ascertained through the detailed correlations to section Giblecemi and the fact that phase relations are known for sapropels in the latter section (Hilgen, 1991a; Hilgen et al., 1995, 2000a; Lourens et al.,

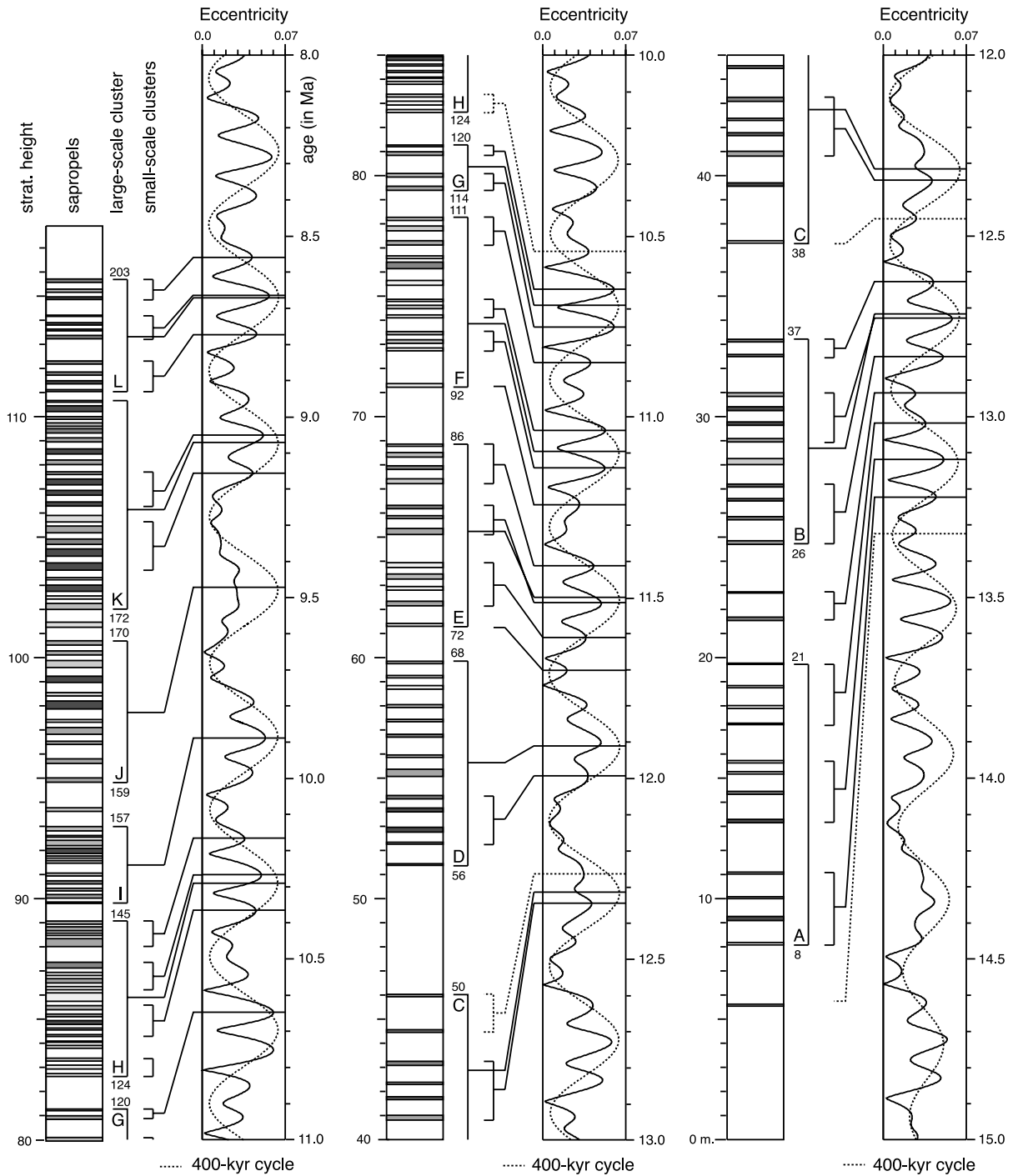


Fig. 10. Tuning of sapropel clusters in the Monte dei Corvi section to eccentricity maxima in the eccentricity time series of solution La90<sub>(1,1)</sub> (Laskar, 1990; Laskar et al., 1993). Small-scale clusters are calibrated to 100-kyr maxima, large-scale clusters (A–L) to 400-kyr maxima.

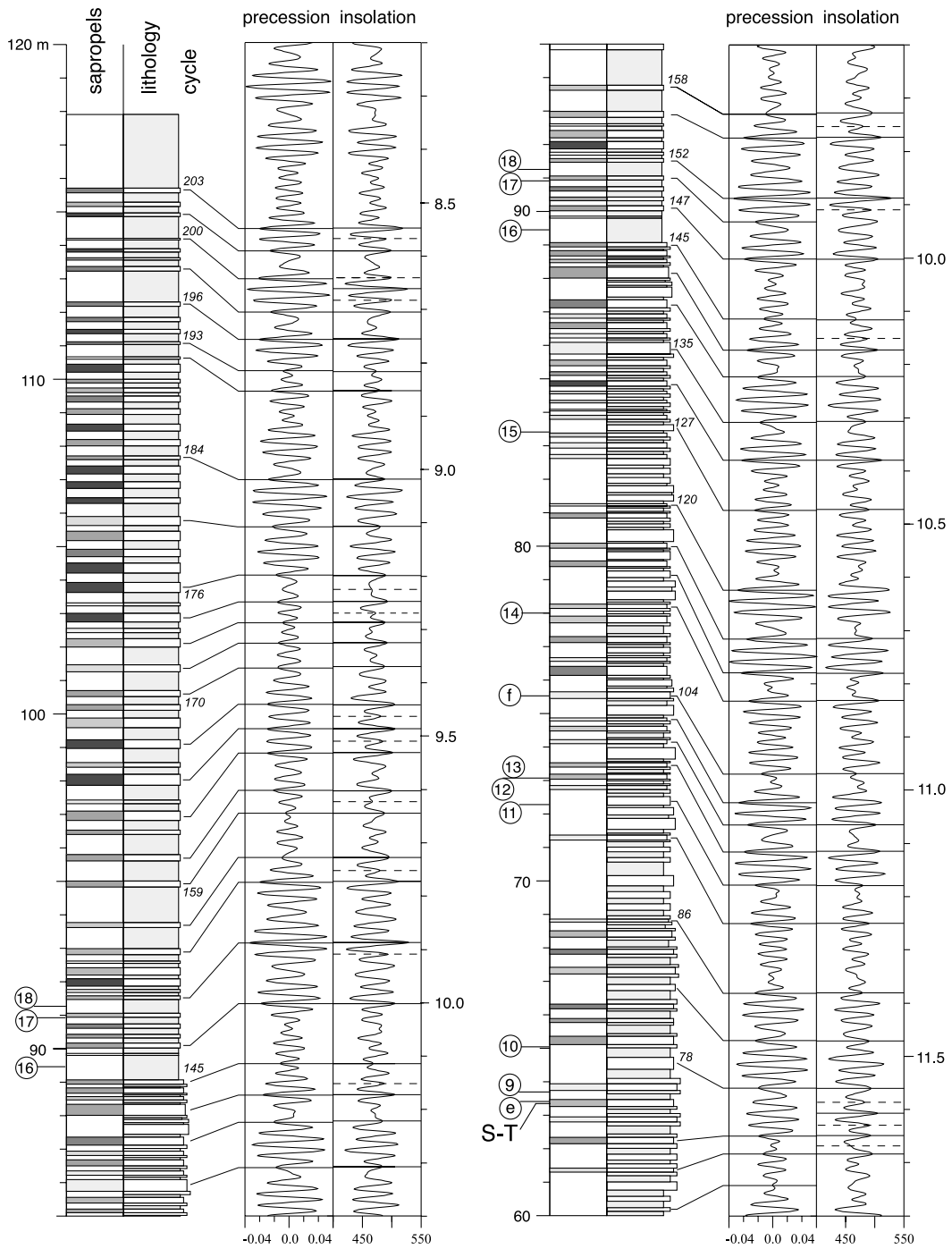


Fig. 11. Detailed tuning of the basic small-scale sedimentary cycles in the upper half of the Monte dei Corvi section to the precession and insolation time series of solution La93<sub>(1,1)</sub>. Also shown are the positions of the calcareous plankton events. Numbers refer to the numbers for the same events in Table 2. S-T indicates the recently proposed Serravallian/Tortonian boundary (Tortonian GSSP).

1996). The observed link between sapropels at Monte dei Corvi and Monte Gibliscemi implies that they correspond to minima in the precession index and, thus, to 65°N lat. (boreal) summer insolation maxima, and that small-scale and large-scale sapropel clusters correspond to 100-kyr and 400-kyr eccentricity maxima, respectively. Finally, alternating thick/thin – or present/absent, or distinct/faint – sapropels in successive basic cycles are related to obliquity maxima/minima and, thus, to high/low-amplitude (boreal) summer insolation maxima, due to precession-obliquity interference.

Using these phase relations and the existing tuning for the sapropels at Monte Gibliscemi as starting point, we first tuned sapropel clusters at Monte dei Corvi to 400-kyr and 100-kyr eccentricity maxima (Fig. 10). Both small-scale and large-scale clusters were identified using differences in visual expression of the sapropels and their preferred occurrence in bundles. To correctly interpret sapropel clusters in terms of eccentricity related patterns, we assumed that a 400-kyr eccentricity cycle corresponds to approximately 20 basic cycles and a 100-kyr cycle to 4–6 basic cycles. In general, recognition of sapropel clusters and the ensuing calibration to eccentricity are straightforward, apart for the interval between 72 and 87 m in which identification of clusters is more problematic. The first-order astronomical calibration of this interval to eccentricity was achieved by taking the number of basic cycles and the detailed correlations to section Gibliscemi in addition into account. Sapropel clusters could again be unambiguously recognized lower in the section (Fig. 10).

The problematic identification of sapropel clusters in the middle part of the section can be explained by difficulties encountered in logging the part of the trajectory underneath the fishermen's sheds and the fact that it corresponds to a maximum in amplitude of the 1.2-Myr obliquity cycle, around 10.8 Ma. In addition, the 400-kyr minimum at 10.9 Ma is weakly developed with relatively high eccentricity values, most likely due to the 2.4-Myr eccentricity maximum around 10.7 Ma. As a consequence, the amplitude of the precession and insolation variations are enhanced for

a prolonged period of time, thus generating conditions that are less favorable for the formation and thus identification of sapropel clusters.

We then succeeded by calibrating the individual basic cycles to precession and insolation starting from the top of the section downward. The resulting tuning is presented in Figs. 11 and 12. It deviates in detail from the astronomical tuning of section Gibliscemi as discussed below. This is not unexpectedly in view of the locally intense deformation at Gibliscemi. Nevertheless, the correlations confirm that Gibliscemi represents a continuous succession despite the deformation.

#### 6.2.1. Cycles 176–203

Cyclostratigraphic correlations between Monte dei Corvi and Monte Gibliscemi are unambiguous in this interval. The initial tuning of Monte Gibliscemi looks convincing but, alternatively, Gibliscemi cycles G33 to G44 may be tuned one precession (insolation) cycle older. A reconnaissance of Monte Gibliscemi (upward extension of section Gibliscemi C, following the trajectory of Sprovieri et al., 1996) revealed the presence of an extra cycle between our cycles G44 and G45 while the remaining homogeneous marlbed remains thicker than the average homogeneous marlbed of regular basic cycles. This implies that the older option is in better agreement with the cyclostratigraphic data (Fig. 11) and thus that the initial tuning of Monte Gibliscemi has to be slightly modified in this interval. The modified tuning is consistent with the almost regular thickness of the homogeneous marlbed between the sapropels of cycles 184 and 185 at Monte dei Corvi, but results in a less good fit with the insolation patterns for cycles 192 to 193.

#### 6.2.2. Cycles 146–176

These cycles can be unambiguously correlated and tuned. The cycle pattern is dominated by basic and intermediate scale cycles and reflects precession/obliquity interference with alternating thick/thin (or present/absent, or distinct/faint) sapropels in successive basic cycles. Clearly, the interference is not perfect over the entire interval, but switches intermittently by one cycle (i.e. at cycles 168–170 and 162–163). However, despite

Table 1a

Astronomical ages of sapropel (or associated calcareous marlbed) midpoint of the basic sedimentary cycles according to the La93<sub>(1,1)</sub> solution (of cycles in the stratigraphic overlap with section Gibliscemi)

Age	MdC	Gib_m	Gib_o
–8548	203	51	51
–8568	202	50	50
–8590	201	49	49
–8619	–	–	–
–8641	200	48	48
–8662	199	47	47
–8683	198	46	46
–8705	197	45	45
–8734	–	–	44
–8756	196	44	43
–8777	195	43	42
–8797	194	42	41
–8816	193	41	–
–8832	–	–	40
–8852	192	40	39
–8872	191	39	38
–8892	190	38	37
–8907	189	37	36
–8926	188	36	35
–8947	187	35	34
–8968	186	34	33
–8990	185	33	–
–9018	184	32	32
–9040	183	31	31
–9061	182	30	30
–9083	181	29	29
–9107	180	28	28
–9133	179	27	27
–9154	178	26	26
–9176	177	25	25
–9198	176	24	24
–9225	175	23	23
–9249	174	22	22
–9269	173	21	21
–9288	172	20	20
–9305	–	–	–
–9325	171	19	19
–9348	–	–	–
–9371	170	18	18

(Continued)

Age	MdC	Gib_m	Gib_o
–9396	169	17	17
–9418	168	16	16
–9440	167	15	15
–9464	166	14	14
–9487	165	13	13
–9510	164	12	12
–9532	163	11	11
–9555	162	10	10
–9580	161	9	9
–9602	160	8	8
–9624	*	–	7
–9644	159	7	6
–9660	*	–	–
–9679	*	6	5
–9700	*	–	4
–9728	158	5	3
–9751	*	4	2
–9773	157	3	1
–9795	156	2	0
–9817	155	1	–1
–9843	154	0	–2
–9866	153	–1	–3
–9888	152	–2	–4
–9909	151	–3	–5
–9932	150	–4	–6
–9959	149	–5	–7
–9980	148	–6	–8
–10002	147	–7	–9
–10023	146	–8	–10
–10041	–	–9	–
–10057	–	–10	–11
–10076	–	–	–12
–10095	–	–11	–13
–10114	145	–12	–14
–10132	144	–13	–15
–10152	143	–14	–16
–10172	142	–15	–
–10193	141	–16	–
–10209	140	–17	–17
–10223	139	–18	–18
–10244	138	–19	–19
–10266	137	–20	–20
–10287	136	–21	–21
–10308	135	–	–22
–10338	134	–22	–23

(Continued)

Age	MdC	Gib_m	Gib_o
–10359	133	–23	–24
–10379	132	–24	–25
–10400	131	–25	–26
–10419	130	–26	–
–10435	129	–	–27
–10453	128	–27	–28
–10473	127	–28	–29
–10492	126	–29	–30
–10511	125	–30	–31
–10530	124	–31	–32
–10550	123	–32	–33
–10570	122	–33	–34
–10586	121B	–34	–
–10602	121A	–35	–35
–10623	120	–36	–36
–10644	119	–37	–37
–10665	118	–38	–38
–10687	117	–	–
–10716	116	–39	–39
–10737	115	–40	–40
–10759	114	–41	–41
–10779	113	–42	–42
–10799	112B	–43	–43
–10812	112A	–	–
–10832	111	–44	–44
–10852	110	–45	–45
–10873	109	–46	–46
–10892	108	–47	–47
–10910	107	–48	–48
–10928	106	–49	–49
–10948	105	–50	–50
–10968	104	–51	–51
–10984	–	–	–
–11002	103	–52	–52
–11023	102	–53	–53
–11043	101	–54	–54
–11064	100	–55	–55
–11093	99	–56	–56
–11116	98	–57	–57
–11137	97	–58	–58
–11158	96	–59	–59
–11178	95	–	–
–11195	–	–	–
–11209	94	–60	–60
–11230	93	–61	–61

(Continued)

Age	MdC	Gib_m	Gib_o
–11251	92	–62	–62
–11270	91	–63	–63
–11289	90	–	–
–11307	–	–	–
–11327	89	–	–
–11346	88	–	–
–11361	87	–64	–64
–11380	86	–65	–65
–11401	85	–66	–66
–11422	84	–67	–67
–11443	83	–68	–68
–11471	82	–69	–69
–11493	81	–70	–70
–11515	80	–71	–71
–11536	79	–72	–72
–11558	78	–73	–73
–11586	77	–74	–74
–11608	76	–75	–75
–11629	75	–76	–76
–11650	74	–77	–77
–11667	73	–	–
–11683	72	–78	–78
–11703	71	–	–
–11723	70	–	–
–11741	69	–	–
–11757	68	–79	–
–11778	67	–80	–79
–11799	66	–	–80
–11821	65	–81	–
–11846	64	–82	–81
–11870	63	–83	–82
–11892	62	–	–83
–11913	61	–84	–
–11936	60A	–	–84
–11961	60	–85	–85
–11984	59	–86	–86
–12006	58	–87	–87

Ages refer to the age of the correlative precession minimum.

Gib\_o shows the ages of the sedimentary cycles at Monte Gibliscemi according to the initial tuning (Hilgen et al., 2000a), Gib\_m shows the ages according to the slightly revised tuning presented in this paper.

Table 1b

Astronomical ages of sapropel (or associated calcareous marlbed) mid-point of the basic sedimentary cycles according to the La93<sub>(1,1)</sub> solution (of older cycles)

Age	MdC	Age	MdC
–12 028	57	–12 761	31
–12 051	56	–12 784	30
–12 077	55	–12 811	29
–12 098	54	–12 832	28
–12 118	53	–12 853	27
–12 137	52	–12 873	26
–12 156	–	–12 892	n.d.
–12 178	–	–12 907	25
–12 202	–	–12 927	24
–12 226	–	–12 947	23
–12 248	51	–12 965	22
–12 270	50	–12 983	21
–12 293	49	–13 003	20
–12 317	48	–13 024	19
–12 340	47	–13 044	18
–12 361	46	–13 062	17
–12 384	45	–13 076	16
–12 407	44	–13 096	15
–12 433	43	–13 117	14
–12 454	42	–13 138	13
–12 474	41	–13 159	12
–12 494	40	–13 175	n.d.
–12 511	39	–13 191	11
–12 531	38	–13 211	10
–12 551	–	–13 232	9
–12 569	–	–13 252	8
–12 583	–	–13 271	7
–12 604	–	–13 288	6
–12 625	37	–13 307	5
–12 646	36	–13 327	4
–12 669	35	–13 345	3?
–12 696	34	–13 363	2?
–12 718	33	–13 382	1?
–12 739	32		

Ages refer to the age of the correlative precession minimum.

its complexity, the cycle pattern shows an almost perfect fit with the insolation target. The excellent fit becomes particularly evident if the parallel section across the beach is taken into account. This section reveals additional ('missing') cycles, which lack the sedimentary expression of a sapropel due to weak insolation forcing, as indurated marlbeds (Fig. 4). The indurated beds are intercalated in homogeneous marls that are thicker than marlbeds of regular basic cycles (Fig. 11).

Despite the unambiguous correlations, the complex cycle pattern is not fully identical to the pat-

tern observed at Monte Gibliscemi. Detailed comparison of the cycle patterns led to a modification of the tuning of the Gibliscemi cycles as follows. Cycles G7/G8, like their counterparts at Monte dei Corvi, must represent double cycles, despite their almost regular thickness in the original log of section Gibliscemi A. Revisiting Monte Gibliscemi showed that the thickness of these cycles varies laterally in section Gibliscemi C, with a systematic increase towards the east, thus rendering support to the alternative interpretation that they represent double cycles. The reduced thickness of these cycles in section Gibliscemi A is at least partly related to deformation which led to a tectonic reduction of this part of the succession. However, the reduced thickness of the same cycles at Monte Giammoia, located some 10 km east of Gibliscemi, and of the overlying cycle (G9) both at Monte Gibliscemi and at Monte Giammoia indicates that a temporary reduction in sedimentation rate must have played a role as well. Despite these complications, the cyclostratigraphic correlations between Monte dei Corvi and Monte Gibliscemi are straightforward and confirmed in detail by the planktonic foraminiferal biostratigraphy.

The dominance of precession/obliquity interference patterns in this interval is related to the minimum in eccentricity of the 2.4-Myr eccentricity cycle reached at 9.5 Ma. During such a minimum, the amplitude of the 100-kyr cycle is strongly reduced, resulting in a relatively low and constant precession amplitude, and precession/obliquity interference in the insolation target (see also Hilgen et al., 1995, 2000c).

### 6.2.3. Cycles 132–146

This is the only interval in which the sedimentary succession might be discontinuous. The marlbed above the sapropel of cycle 145 contains several rounded sapropel 'flakes' embedded in an otherwise homogeneous marl. In principle, such rounded components can either be explained by resedimentation or by burrows filled with sapropelitic sediment. Our detailed bed-to-bed correlations to Monte Gibliscemi indicate that the Monte dei Corvi section contains less cycles in the interval from cycle 136 to 146 than the corre-

relative interval at Monte Gibliscemi (Fig. 9). More specifically our correlations show that cycles G-11 to G-9 (or G-8) lack sedimentary expression at Monte dei Corvi. The lack of sedimentary expression of these cycles can be explained by the low amplitude of the precession/insolation forcing in this interval which corresponds to the 400-kyr eccentricity minimum around 10.1 Ma. But in that case it remains unexplained why the correlative sapropel of the prominent cycle G-11 is not developed. Alternatively, the section might be punctuated by a hiatus with a maximum duration of 80 kyr. In that case, the thick homogeneous marlbed of cycle 145 is interpreted as a slump level and the hiatus placed at the base of this bed. Nevertheless, we consider the former option that the homogeneous marlbed represents normal marine pelagic sedimentation more likely because no further indications for a sedimentary slump were found in the homogeneous marlbed of cycle 145. Note that cycles 140–145 can equally well be tuned one precession-insolation cycle younger.

To overcome the potential problem of the hiatus, we continued with the tuning of Monte Gibliscemi to older levels until cycles were reached that could be unambiguously correlated to Monte dei Corvi again on the basis of the cycle patterns (136 to 139 that correlate with G-18 to G-21). Evidently, these older cycles reflect precession-obliquity interference. The tuning of these cycles however is less straightforward because the interference pattern is not manifest in the insolation target, even if an uncertainty of one or two cycles in the tuning is assumed (Fig. 9). The most likely explanation for this discrepancy is that details, such as precession/obliquity interference, become less reliable in our preferred solution  $La93_{(1,1)}$  (Laskar, 1990; Laskar et al., 1993), because major uncertainties in the tuning can be excluded. The interference pattern as can be inferred from the sedimentary cyclicity only becomes visible after a significant reduction of the (present-day) tidal dissipation term from 1 to 0.5 (or an equivalent reduction in the dynamical ellipticity). But, in that case, the almost excellent fit with insolation gets lost for the interval encompassing cycles 146–176. As a consequence, details in the insolation time series reflecting precession/obliquity interference

can no longer be employed with certainty for the tuning of older cycles.

#### 6.2.4. Cycles 86–132

This interval includes the difficult and problematic passage beneath the fisherman's sheds. We preferred to log this trajectory instead of the trajectory followed by Montanari et al. (1997b) above the sheds, because the latter trajectory is more weathered. This stronger weathering explains the almost complete lack of sapropels in their log of the same interval.

The tuning of this interval is difficult in so far that the basic cycle patterns do not allow to distinguish sapropel clusters in a routine way, as mentioned in the section on the first-order astronomical calibration to eccentricity. The detailed tuning to precession is based on the number of basic cycles, the tuning of the interval stratigraphically directly below and above, and the tuning of the correlative part of the Gibliscemi section. In addition, the identification of basic cycles showing a minimum contrast in lithology that correspond to 100-kyr eccentricity minima played an important role in the tuning of this interval (cycles 99, 103, 112, 117 and 121). Intricate details of the cycle pattern reflecting precession/obliquity interference are not observed in the insolation target.

#### 6.2.5. Cycles 52–86

The tuning of the basic cycles to precession is straightforward. No good match with insolation is found, however, most likely because precession/obliquity interference is not reliably resolved in this interval (see above).

#### 6.2.6. Cycles 37–52

The detailed tuning of these cycles is complicated because they are sandwiched in between the two thick intervals (I and II) in which the basic small-scale cyclicity could not be resolved in the field and which correspond to two successive 400-kyr eccentricity minima at 12.15 and 12.55 Ma. In principle, this shortcoming could have been overcome because the sapropel pattern is very characteristic and dominated by precession-obliquity interference. However, as stated above, it is unlikely that such interference patterns

are reliably resolved in La93<sub>(1,1)</sub> this far back in time. As a consequence, several options exist for the tuning of cycles 38–51. The small-scale sapropel cluster of cycles 43–46 can be calibrated to the most distinct albeit weakly developed 100-kyr eccentricity maximum at 12.35 Ma. Using this constraint, the cycles 38–51 can be tuned in one way only (Fig. 12). But an alternative option is to correlate these cycles one or two precession cycles

older (see also Fig. 12). The latter preferred tuning is based on ongoing studies of parallel sections on San Nicola Island (Tremi islands, Adriatic Sea, Italy) in which the cyclostratigraphy of the problematic intervals I and II is better resolved (unpublished data).

Dominance of precession–obliquity interference over the precession/eccentricity syndrome is associated with the minimum in eccentricity related to

Table 2

Astronomical ages of calcareous plankton bioevents in the Monte dei Corvi section and comparison with the ages of the same events in section Gibilscemi and in other sections from the Mediterranean

No. Species	Event	Cycle	Position	MdC age	MG age	RIPS (2002)
<b>Planktonic foraminifer</b>						
18 <i>Neogloboquadrina</i> group	s/d	150–152	91.00–91.525	9.888–9.932	–	–
17 <i>Globorotalia partimlabiata</i>	LO	150	90.84–91.00	9.932–9.945	9.913 ± 0.003	[11.80]
16 <i>Neogloboquadrina</i> group	d/s	145	89.005–89.82	10.024–10.114	10.011 ± 0.002	–
15 <i>Neogloboquadrina atlantica</i> s.s.	LRO	126–127	83.32–83.54	10.473–10.492	10.473 ± 0.001	–
– <i>Neogloboquadrina acostaensis</i> s.s.	FRO	–	–	–	10.554 ± 0.003	10.55
14 <i>Neogloboquadrina atlantica</i> l.s.	LO	110	77.81–78.205	10.832–10.852	10.850 ± 0.002	–
13 <i>Neogloboquadrina atlantica</i> l.s.	FO	96–97	72.95–73.11	11.137–11.148	11.121 ± 0.003	11.15
12 <i>Neogloboquadrina</i> group	2nd influx	96–97	72.95–73.11	11.137–11.148	11.178 ± 0.003	–
11 <i>Paragloborotalia siakensis</i>	LO	94–95	72.225–72.39	11.178–11.195	11.205 ± 0.004	11.21
10 <i>Globoturborotalita apertura–Globigerinoides obliquus</i> gr.	FRO	78–79	64.87–65.18	11.538–11.548	–	11.54
9 <i>Globigerinoides subquadratus</i>	LCO	76–77	63.555–63.84	11.586–11.599	11.539 ± 0.004	11.54
8 <i>Neogloboquadrina</i> group	FO	67–68	59.55–59.80	11.757–11.766	11.781 ± 0.002	11.80
7 <i>Paragloborotalia siakensis</i>	IIAE	57–58	52.70–52.86	12.006–12.012	–	12.00
6 <i>Paragloborotalia mayeri</i>	LO	56	51.345–51.54	12.048–12.055	–	12.14
5 <i>Paragloborotalia siakensis</i>	IIAB	42	40.09–40.48	12.444–12.454	–	12.38
4 <i>Paragloborotalia siakensis</i>	IAE	37	33.155–33.735	12.612–12.625	–	12.58
3 <i>Globorotalia partimlabiata</i>	FO	30	28.135–28.685	12.770–12.784	–	12.62
2 <i>Paragloborotalia mayeri</i>	F(C)O	30	28.135–28.685	12.770–12.784	–	12.34
1 <i>Paragloborotalia siakensis</i>	IAB	4–5	5.295–5.58	13.307–13.313	–	13.22
<b>Calcareous nannofossil</b>						
– <i>Discoaster neohamatus</i>	FO	–	–	–	9.826 ± 0.003	–
– <i>Discoaster hamatus</i>	FO	–	–	–	10.150 ± 0.002	–
– <i>Helicosphaera stalis</i>	FCO	–	–	–	10.717 ± 0.002	10.71
– <i>Catinaster coalitus</i>	FO	–	–	–	10.738 ± 0.001	10.74
– <i>Helicosphaera walbersdorfensis</i>	LCO	–	–	–	10.743 ± 0.003	10.76
f <i>Coccolithus miopelagicus</i>	LRO	104	75.55	10.968	10.977 ± 0.002	11.18/19
e <i>Discoaster kugleri</i>	LCO	76	63.365–63.555	11.599–11.608	11.604 ± 0.002	11.60
d <i>Discoaster kugleri</i>	FCO	61	55.13–55.31	11.910–11.917	11.889 ± 0.004	11.90
c <i>Calcidiscus premacintyreii</i>	L(C)O	44–45	42.065–42.335	12.384–12.394	–	12.51
b <i>Calcidiscus macintyreii</i>	FO	43–44	41.355–41.72	12.407–12.419	–	12.57
a <i>Cyclicargolithus floridanus</i>	L(C)O?	6–7	7.05–7.89	13.259–13.279	–	13.39

We calculated ages of individual samples by means of linear interpolation between succession age calibration points. As calibration points we used the ages of precession minima and assigned them to the correlative sapropel mid-point. We used the mid-point of the corresponding limestone bed for cycles which do not have a sapropel. We assigned the age to the base of limestone bed if no sapropel is present and only limestone bed B developed as is the case in a limited number of cycles from the lower part of the section.

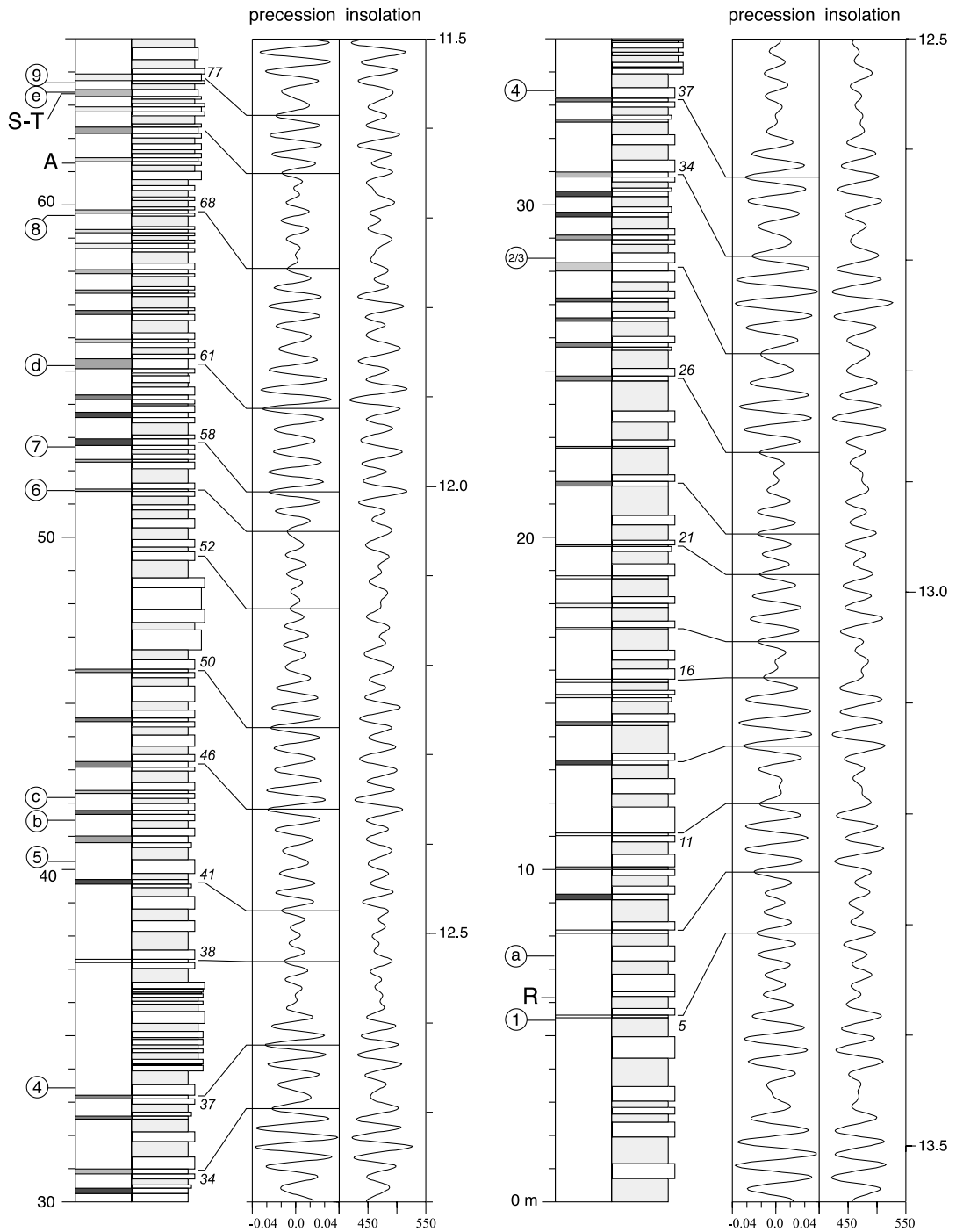


Fig. 12. Detailed tuning of the basic small-scale sedimentary cycles in the lower half of the Monte dei Corvi section to the precession and insolation time series of solution La93<sub>(1,1)</sub>. Also shown are the positions of the calcareous plankton events. Numbers refer to the numbers for the same events in Table 2. R and A indicate the Respighi and Ancona ashbeds. S-T indicates the recently proposed Serravallian/Tortonian boundary (Tortonian GSSP).

Table 3  
Astronomical ages of magnetic reversals in the Monte dei Corvi section and comparison with (and difference in) ages for the same reversals in the Gibliscemi, Meto-  
chia and Orera sections and according to CK95

Reversal	Position	Cycle	Astronomical age	Gib <sub>mod</sub>	Met	$\Delta$	Orera	$\Delta$	CK95	$\Delta$
C4r.2r-1 (y)	113.58–114.01	198/199	8.668 (8.652–8.684)	–	8.662 (8.651–8.673)	6	–	–	8.635	33
C4r.2r-1 (o)	113.09–113.58	196/198	8.700 (8.684–8.715)	–	8.705 (8.697–8.713)	–5	–	–	8.651	49
C4An (y)	111.55–111.93	194/195	8.780 (8.770–8.790)	–	–	–	–	–	8.699	81
C4An (o)	106.11–107.44	180/183	9.062 (9.031–9.093)	–	–	–	–	–	9.025	37
C4Ar.1n (y)	100.32–101.14	169/170	9.364 (9.339–9.388)	9.277 (9.255–9.299)	–	87	–	–	9.230	134
C4Ar.1n (o)	98.92–99.91	166/168	9.428 (9.410–9.447)	9.407 (9.384–9.430)	x	21	–	–	9.308	120
C4Ar.2n (y)	93.97–94.63	158/extra	9.687 (9.664–9.709)	9.669 (9.657–9.676)	x	18	–	–	9.580	107
C4Ar.2n (o)	93.34–93.97	157/158	9.729 (9.709–9.748)	9.727 (9.721–9.733)	x	2	–	–	9.642	87
C5n.1n (y)	92.62–93.34	156/157	9.770 (9.748–9.793)	–	–	–	–	–	9.740	30
C5n.1n (o)	91.27–92.12	150/154	9.871 (9.832–9.909)	–	–	–	–	–	9.880	–9
C5n.2n (y)	89.72–90.48	145/148	10.004 (9.973–10.035)	–	–	–	–	–	9.920	84
C5r.2r-1 (y)	71.09–71.92	91/93	11.240 (11.218–11.262)	–	–	–	11.251	–11	–	–
C5r.2r-1 (o)	70.25–71.09	89/91	11.287 (11.262–11.312)	–	–	–	11.280	7	–	–

Ages for reversals in section Gibliscemi have been recalculated following the slightly modified tuning of the cycles proposed in the present paper.

the 2.4-Myr cycle around 12.2 Ma (Fig. 9). This relationship is similar to that observed for the interval which encompasses cycles 150–176 and corresponds to the next younger 2.4-Myr eccentricity minimum.

### 6.2.7. Cycles 4–37

Despite the uncertainty in the tuning of cycles 38–51, the tuning of cycles 4–37 to precession is unambiguous again. This is due to the application of the larger-scale eccentricity related cycles for a first-order astronomical tuning, thus preventing a downward accumulation of errors in the tuning. In this case, the potential error in the tuning is even eliminated because there is only one option for the tuning of the sapropels in the small-scale clusters of large-scale clusters A and B to precession. The age for the base of our section arrives at 13.4 Ma.

## 7. Discussion

The astronomical tuning in combination with the integrated stratigraphic correlations to section Gibliscemi reveal that the Monte dei Corvi section is continuous within the resolution of the applied cyclostratigraphic framework, except for the presence of a possible hiatus with a maximum duration of 80 kyr in the Tortonian. Our initial concern about the continuity of the section based on the absence of the first neogloboquadrinid influx and the *D. kugleri* acme remains unwarranted. The different biostratigraphic outcome of the present study, which does reveal the presence of both the first neogloboquadrinid influx as well as the *D. kugleri* acme must be explained by a combination of sample density, preservation, taxonomic concept and rarity of marker species. Typical *D. kugleri* was initially reported to be absent (Montanari et al., 1997b) but re-examination of the samples revealed that rare and atypical specimens similar to *D. kugleri* are present in a limited number of samples directly below the Ancona ashbed (D. Rio and E. Fornaciari, pers. comm.). Unfortunately, a more detailed analysis was hampered by the scarceness of discoasterids in combination with the generally poor preserva-

tion of the calcareous nannofossils. Like in section Gibilscemi, typical *N. acostaensis* is rare in the interval marked by the first neogloboquadrinid influx and can easily be missed when preservation is moderate to poor as in Monte dei Corvi. The other neogloboquadrinids (small-sized *N. atlantica* and four-chambered morphotypes) have most likely been included in *P. continuosa* by Montanari et al. (1997b).

### 7.1. Astronomical time scale

The tuning provides astronomical ages for all sedimentary cycles, calcareous plankton bioevents and magnetic reversals recorded in section Monte dei Corvi (Tables 1a,b–3). Ages of bioevents are in good to excellent agreement with tuned ages obtained for the same events in the Gibilscemi and Case Pelacani sections (Hilgen et al., 2000a; Caruso et al., 2002) but differ from ages in parallel sections in the Mediterranean for the time interval older than 12 Ma (Table 2, see discussion below). Comparison with the tuned ages for the same events at Ceara Rise confirms previous notions of a strong diachrony of some important zonal marker events, such as the FO of the neogloboquadrinids and the LO of *P. mayeri*, and the almost perfect synchrony of other events, such as the FO and LCO of *D. kugleri* and the *G. subquadratus* LCO.

The astronomical ages for the magnetic reversals in the younger part of the section are in good agreement with astronomical ages for the same reversals in the Gibilscemi and Metochia sections (Table 3) apart from C4Ar.2n(y) which is significantly younger. The present study in addition provides direct astronomical ages for reversals

that were not recorded in the latter sections due to adverse magnetic properties. Unfortunately, the lower half of the Monte dei Corvi section did not provide a reliable magnetostratigraphy although several short intervals with reversed polarities and a single short interval with normal polarities were recorded. Astronomical ages for the short normal polarity interval overlap with tuned ages for a normal polarity interval in the continental Orera section in Spain that corresponds to cryptochron C5r.2r-1n (Abdul Aziz et al., 2003). Tuned ages for the intervals of reversed polarity are consistent with the astronomically dated magnetic reversal history of Orera (Abdul Aziz et al., 2003); these intervals correspond to (parts of) C5r.3r, C5An.1r and C5Ar.1r. The results of the present study in combination with the tuned magnetostratigraphy of the Orera section result in the completion of the astronomical polarity time scale for the last 13 Myr.

The tuning in addition provides ages for the Ancona and Respighi ash layers that have previously been dated by  $^{40}\text{Ar}/^{39}\text{Ar}$  incremental heating experiments on biotites at 11.43 and 12.86 Ma, respectively (Montanari et al., 1997b). The astronomical and  $^{40}\text{Ar}/^{39}\text{Ar}$  ages are compared with one another in Table 4. This comparison confirms earlier notions that astronomical ages are older than the  $^{40}\text{Ar}/^{39}\text{Ar}$  ages, at least if previously widely accepted ages for mineral dating standards are used. The discrepancy is reduced but not completely eliminated if revised, older ages for the monitor dating standard (Fish Canyon Tuff sanidine) are applied (Renne et al., 1998). The astronomical ages would fit with an age of  $\sim 28.50$  Ma for the FCT which is in remarkable good agreement with the U/Pb age of

Table 4

Astronomical ages of the Ancona and Respighi ashbeds and comparison with  $^{40}\text{Ar}/^{39}\text{Ar}$  ages of biotites from the same ash layers

Ash layer	Ar/Ar			Astronomical age		
	27.84	28.02	28.50	Cleveland	Revised	Ours
Ancona	11.43	11.50	11.70	11.56	11.67	11.688
Respighi	12.86	12.94	13.16	12.98	13.28	13.296
	12.94*	13.02*	13.25*			

Biotite ages have been calculated using ages of 27.84, 28.02 and 28.50 Ma for the FCT-san monitor dating standard. Revised ages of Cleaveland et al. (2002) based on the modified tuning presented in Fig. 13. Asterisks indicate ages for the Respighi ash if the slightly discrepant oldest age is included in the calculation (see Montanari et al., 1997b).

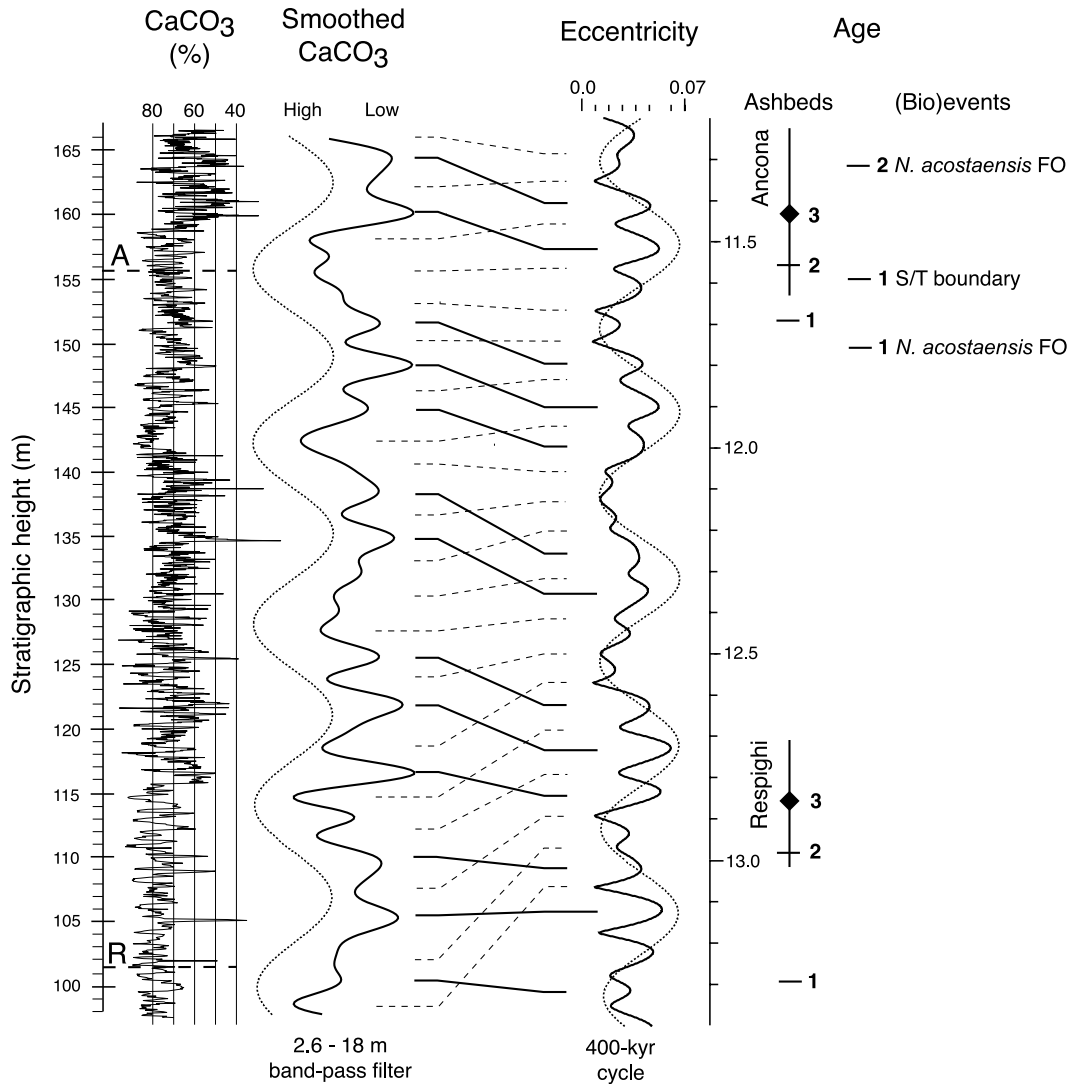


Fig. 13. Correlation of the low-frequency variations in  $\text{CaCO}_3$  content (of Cleaveland et al., 2002) in the lower part of the Monte dei Corvi Beach section to the eccentricity time series of solution La93. Both the initial tuning of Cleaveland et al. (2002); (dashed lines) as well as our revised tuning (solid lines) are shown. Both assume that  $\text{CaCO}_3$  maxima correspond to eccentricity minima, i.e. similar to the observed phase relation in the Pliocene Trubi Formation on Sicily (Hilgen, 1991b). The smoothed  $\text{CaCO}_3$  record is based on applying a bandpass filter with a 2.6–18 m width to the  $\text{CaCO}_3$  depth series shown to the left (see Cleaveland et al., 2002). In addition the large-scale  $\text{CaCO}_3$  cycle related to 400-kyr eccentricity has been schematically indicated (dotted line). Note that the tuning of Cleaveland et al. (2002) is consistent with the radiometric ages of the ashbeds and that our tuning is consistent with the 400-kyr eccentricity cycle. Ages of the Ancona (A) and Respighi (R) ashbeds are indicated to the right as follows: 1. astronomical age, this paper; 2. astronomical age of Cleaveland et al. (2002), and 3.  $^{40}\text{Ar}/^{39}\text{Ar}$  biotite age of Montanari et al. (1997b). Also indicated are the ages for the *N. acostaensis* FO (1. our age; 2. astronomical age of Cleaveland et al., 2002) and our astronomical age of the Serravallian/Tortonian (S/T) boundary according to a recent proposal to define the Tortonian GSSP close to the *D. kugleri* and *G. subquadratus* LCOs in the Monte dei Corvi section (Hilgen et al., 2003).

Schmitz and Bowring (2001) but which is inconsistent with previous attempts to intercalibrate radioisotopic and astronomic time (Renne et al., 1994; Hilgen et al., 1997; Steenbrink et al., 1999). Clearly more research is needed to solve this fundamental problem in geochronometry.

### 7.2. Alternative tunings

Our tuning deviates from the tuning of the low-frequency variations in a high-resolution carbonate record from the lower part of the Monte dei Corvi Beach section to eccentricity proposed by Cleaveland et al. (2002). Their tuning, which is within error consistent with the  $^{40}\text{Ar}/^{39}\text{Ar}$  biotite ages of the ash layers, is based on correlating successive carbonate maxima to 100-kyr eccentricity minima but is less convincing when the 400-kyr cycle is examined. In fact their tuning can be easily adjusted as to make it consistent with ours (see below). The inconsistency in their tuning partly results from their wish to stay within error to the published biotite ages while we could extend our existing tuning for the younger part of the Mediterranean Miocene. Our alternative tuning for the low-frequency variations in carbonate content to eccentricity is presented in Fig. 13. This tuning results in a much better fit with the 400-kyr eccentricity cycle and seems consistent with our ages for the ash layers. The large discrepancy in the tuned ages for the *N. acostaensis* FO is explained by the fact that the first neogloboquadrid influx was not recorded by Montanari et al. (1997b).

An apparent misfit in the revised tuning is found slightly above the Ancona ashbed in the interval between 157 and 160 m (Fig. 13) where a distinct carbonate maximum corresponds to increasing eccentricity values following the 400-kyr minimum at 11.7 Ma. This misfit is recognizable in the field as the first prominent cape east of the fishermen's sheds. This small cape represents the carbonate maximum but it also contains the small-scale sapropel cluster of cycles 74–77 that correlates with the 100-kyr eccentricity maximum at 11.62 Ma. This interval coincides with the oxygen isotope event Mi-5 as recorded in section Glibiscemi (Turco et al., 2001), suggesting that this

event exerted an additional control on the carbonate content in this particular interval.

Discrepant ages of the calcareous plankton events (Table 2) indicate that our tuning must also deviate from the tuning of parallel sections in the Mediterranean, which together cover the time interval between 10.5 and 13.7 Ma (Case Pelacani, Caruso et al., 2002; Tremiti, Lirer et al., 2002; Ras il-Pellegrin, Sprovieri et al., 2002a). However, at this stage, it is difficult to compare both these tunings in detail because of the different biostratigraphic methods applied and the limited reliability of several events in the critical interval due to the rare and scattered presence of the marker species. When the ages of the more reliable events (*D. kugleri* FCO and LCO, *Neogloboquadrina* group FO, *P. siakensis* IAB, IAE, IIAB, IIAE and *G. partimlabiata* FO) are compared, it is clear that the tuning is essentially consistent back to 12 Ma but that it starts to deviate for older time intervals with a maximum discrepancy of 160 kyr for the *G. partimlabiata* FO (Table 2). The tuning of the Tremiti sections in the critical interval is based on cycle counts rather than on cycle patterns, although eccentricity related signals are taken into account as a check on the precession tuning. The latter is crucial for avoiding the accumulation of errors in the more subjective cycle counts by tracing the expression of the eccentricity envelope of the precession amplitude. On Tremiti, cycle counts are complicated by the presence of an hiatus (work in progress), the lack of sedimentary expression of some basic cycles and their complex quadripartite build-up with often two carbonate minima (one red and one gray) per cycle instead of one as assumed by Lirer et al. (2002). Moreover, the tuning is based on less well exposed and therefore less suitable sections located on opposite sites of San Nicola Island while an ideal composite section can be constructed using the excellent but difficult to reach exposures along the steep northwest facing cliffs. Finally, a potential error lies in the reliability of the two biostratigraphic events, the *P. mayeri* FCO and the *C. premaxintyreii* LCO, used as timelines to correlate Tremiti to the older Ras il-Pellegrin section on Malta and extend the tuning further downward.

Although the discrepancies are rather small from a geological perspective they have important consequences for – the consistency of – phase relations between the sedimentary cyclicity and the astronomical parameters, and pose serious limitations for studies that aim to reconstruct the effects of astronomical climate forcing. The results of our study indicate that a single orbital induced oscillatory climate system can be held responsible for Neogene sapropel formation in the Mediterranean over the last 13.5 million years. A recent climate modeling experiment of orbital extremes indicates that the African monsoon is at least partly responsible (Tuenter et al., 2003), thereby confirming earlier ideas of Rossignol-Strick (1983) and Prell and Kutzbach (1987). In addition this study provides support for the use of the classical 65°N lat. summer insolation curve as a tuning target by demonstrating an obliquity control on the African monsoon intensity mostly via summer heating of the Eurasian continent at latitudes higher than 30° or even 50° (Tuenter et al., 2003).

### 7.3. GSSPs, APTS and astronomical solutions

Summarizing the demonstrable continuity of the succession in the Serravallian–Tortonian boundary interval in combination with the astronomical tuning of the cycles strengthens the case for Monte dei Corvi as a candidate for defining the Tortonian GSSP as proposed by Montanari et al. (1997b) and Odin et al. (1997), who in addition suggested to define the Serravallian and Messinian GSSPs in the same section. Serious shortcomings are the moderate to poor preservation of the calcareous plankton, the lack of a reliable magnetostratigraphy in the lower half of the section and, in case of the Serravallian GSSP, the accessibility of the Monte dei Corvi High Cliff section, which was not included in the present study. The Messinian GSSP has recently been defined at the base of astronomically dated color cycle no. 15 in section Oued Akrech, located on the Atlantic side of Morocco (Hilgen et al., 2000b,c). Recently it has been proposed to formally define the Tortonian GSSP in the Monte dei Corvi section at the mid-point of the sapropel of cycle 76 ([www.geo.uu.nl/SNS](http://www.geo.uu.nl/SNS)). This level coincides closely

with the LCOs of *D. kugleri* and *G. subquadratus*; these events are demonstrable (near)synchronous between the Mediterranean and low-latitude ocean (Hilgen et al., 2000a).

Despite the moderate to poor preservation, detailed biostratigraphic correlations to section Glibiscemi – characterized by a much better preservation – were possible, but the preservation conditions certainly hampers to establish a reliable stable isotope record. The lack of a reliable magnetostratigraphy in the Serravallian–Tortonian boundary interval can be overcome within the framework of an astronomically tuned integrated stratigraphy because a single tuned section with a reliable magnetostratigraphy is sufficient to bridge the gap. Tuned ages for reversal boundaries are not yet available for this interval from the marine record but they have been obtained from the continental Orera section in Spain (Abdul Aziz et al., 2003).

Finally, the unambiguous tuning of the upper part of the section, reflecting precession–obliquity interference, offers an excellent opportunity for a very detailed comparison between the intricate cycle patterns and different astronomical solutions. The almost perfect fit suggests that the ideal solution must be close to solution La93<sub>(1,1)</sub> with present-day values for the dynamical ellipticity of the Earth and the tidal dissipation by the Moon. This outcome is in line with previous studies directed at testing the accuracy of astronomical solutions by means of a detailed statistical comparison with sedimentary archives of the orbital forcing of past climate (Lourens et al., 1996, 2001; Pälike and Shackleton, 2000). But it is also clear from the present study that serious misfits start to arise for intervals older than 10 Ma. To explain these misfits we have compared the cycle patterns with the same insolation target curve derived from the La90-93 solution but with different values for tidal dissipation. Neither of these curves produced an excellent and convincing fit with all cycle patterns in the Monte dei Corvi Beach section although the differences in the ages of the insolation peaks remain very small in the order of 1–10 kyr. Consequently the misfits are difficult to explain other than by small uncertainties in the astronomical solution itself. A

detailed comparison with a new numerical solution may reveal whether this is indeed the case.

## 8. Conclusions

The distinct cycle patterns and the calcareous plankton biostratigraphy and magnetostratigraphy allow the Monte dei Corvi section to be astronomically tuned by correlating sedimentary cycles to the precession and insolation time series of the La93<sub>(1,1)</sub> solution. The tuning is unambiguous for the younger part of the section but may be off in parts by one or occasionally even two cycles in older parts. Intervals marked by the near-absence of small-scale sapropel clusters related to the 100-kyr eccentricity cycle and prolonged dominance of the intermediate cycle and thus precession–obliquity interference correspond to minima in eccentricity related to the 2.4-Myr eccentricity cycle. Our tuning marks a significant improvement of the recently published astronomical calibrations of the Monte dei Corvi section (Cleaveland et al., 2002) and of parallel sections in the Mediterranean (Lirer et al., 2002; Sprovieri et al., 2002a).

Astronomical ages for the reversal boundaries in combination with the tuned magnetostratigraphy of the continental Orera section in Spain (Abdul Aziz et al., 2003) results in the completion of the astronomical polarity time scale for the last 13 Myr. Tuned ages for the Ancona and Respighi ash layers are significantly older (by 250–400 kyr) than published <sup>40</sup>Ar/<sup>39</sup>Ar biotite ages reported for the same layers.

Finally, our study reveals that the Monte dei Corvi Beach section is an acceptable candidate for defining the Tortonian GSSP, despite its obvious shortcomings, and that a single orbital induced oscillatory system is responsible for late Neogene sapropel formation in the Mediterranean by continuously affecting (circum-)Mediterranean climate throughout the last 13.5 million years.

## Acknowledgements

Silvia Iaccarino and Willem-Jan Zachariasse

are thanked for discussion and constructive reading of the manuscript. Alessandro Montanari and David Bice gratefully sent and discussed the electronic version of figure 3 of the Cleaveland et al. paper. We are further thankful to Maria-Bianca Cita, Rudolfo Sprovieri and Finn Surlyk for their critical reviews which considerably improved the manuscript. Esther van Assen, Tanja Kouwenhoven and Erwin van der Laan are thanked for their help in the field, Esther in particular for constructing ‘Dutch’ dams to facilitate logging of the problematic part of the trajectory underneath the fishermen’s sheds. Unfortunately, the dams were repeatedly destroyed by bow waves of the ferries.

## References

- Abdul Aziz, H., Hilgen, F.J., Krijgsman, W., Calvo, J.P., Wilson, D.S., 2003. An astronomical polarity time scale for the late middle Miocene based on cyclic continental sequences. *J. Geophys. Res.* 108, B3 2159.
- Backman, J., Raffi, I., 1997. Calibration of Miocene nannofossil events to orbitally-tuned cyclostratigraphies from Ceara Rise. *Proc. ODP Sci. Res.* 154, 83–99.
- Blow, W.H., 1969. Late middle Eocene to Recent planktonic foraminiferal biostratigraphy. In: Bronniman, P., Renz, H.H. (Eds.), *Proc. First. Int. Conf. Planktonic Microfossils*, Geneva, 1967, Vol. 1. E.J. Brill, Leiden, pp. 199–422.
- Bolli, H.M., 1957. Planktonic foraminifera from the Oligocene-Miocene Cipro and Lengua Formations of Trinidad, B.W.I. In: Loeblich, A.R., et al. (Eds.), *Studies in Foraminifera*. US Nat. Mus. Bull. 215, 97–123.
- Bolli, H.M., Saunders, J.B., 1985. Oligocene to Holocene low latitude planktic foraminifera. In: Bolli, H.M., Saunders, J.B., Perch-Nielsen, K. (Eds.), *Plankton Stratigraphy*. Cambridge University Press, pp. 155–262.
- Cande, S.C., Kent, D.V., 1995. Revised calibration of the Geomagnetic Polarity Time Scale for the Late Cretaceous and Cenozoic. *J. Geophys. Res.* 100, 6093–6095.
- Caruso, A., Sprovieri, M., Bonanno, A., Sprovieri, R., 2002. Astronomical calibration of the Serravallian-Tortonian Case Pelacani section (Sicily, Italy). In: Iaccarino, S. (Ed.), *Integrated Stratigraphy and Paleooceanography of the Mediterranean Middle Miocene*. *Riv. Ital. Paleontol. Stratigr.* 108, 297–306.
- Cleaveland, L.C., Jensen, J., Goese, S., Bice, D.M., Montanari, A., 2002. Cyclostratigraphic analysis of pelagic carbonates at Monte dei Corvi (Ancona, Italy) and astronomical correlation of the Serravallian-Tortonian boundary. *Geology* 30, 931–934.

- Coccioni, R., Di Leo, C., Galeotti, S., 1992. Planktonic foraminiferal biostratigraphy of the upper Serravallian-lower Tortonian Monte dei Corvi section (Northeastern Apennines, Italy). In: Montanari, A., et al. (Eds.), Conferenza Interdisciplinare di Geologia sull'Epoca Miocenica con Enfasi sulla Sequenza Umbro-marchigiana, Ancona, 1992. Miocene Columbus Project (I.U.G.S.). Abstracts and Field Trips, pp. 53–56.
- Coccioni, R., Galeotti, S., Di Leo, R., 1994. The first occurrence of *Neoglobobadrina atlantica* (Berggren) in the Mediterranean. *Giorn. Geol.* 56, 127–138.
- Di Stefano, E., Bonomo, S., Caruso, A., Dinares-Turell, J., Foresi, L.M., Salvatorini, G., Sprovieri, R., 2002. Calcareous plankton bio-events in the Miocene Case Pelacani section (southeastern Sicily, Italy). *Riv. Ital. Paleontol. Stratigr.* 108, 307–323.
- Foresi, L.M., Iaccarino, S., Mazzei, R., Salvatorini, G., 1998. New data on Middle to Late Miocene calcareous plankton biostratigraphy in the Mediterranean area. *Riv. Ital. Paleontol. Stratigr.* 104, 95–114.
- Foresi, L.M., Bonomo, S., Caruso, A., Di Stefano, A., Di Stefano, E., Iaccarino, S.M., Lirer, F., Salvatorini, G., Sprovieri, R., 2002a. High-resolution calcareous plankton biostratigraphy of the Serravallian succession of the Tremiti Islands (Adriatic Sea, Italy). In: Iaccarino, S. (Ed.), Integrated Stratigraphy and Paleocyanography of the Mediterranean Middle Miocene. *Riv. Ital. Paleontol. Stratigr.* 108, 257–273.
- Foresi, L.M., Bonomo, S., Caruso, A., Di Stefano, E., Salvatorini, G., Sprovieri, R., 2002b. Calcareous plankton high-resolution biostratigraphy (foraminifera and calcareous nanofossils) and cyclostratigraphy of the Uppermost Langhian-Lower Serravallian Ras Il-Pellegrin section (Malta). In: Iaccarino, S. (Ed.), Integrated Stratigraphy and Paleocyanography of the Mediterranean Middle Miocene. *Riv. Ital. Paleontol. Stratigr.* 108, 195–210.
- Foresi, L.M., Iaccarino, S., Salvatorini, G., 2002c. *Neoglobobadrina atlantica praeatlantica*, new subspecies from Late Middle Miocene. In: Iaccarino, S. (Ed.), Integrated Stratigraphy and Paleocyanography of the Mediterranean Middle Miocene. *Riv. Ital. Paleontol. Stratigr.* 108, 325–336.
- Foresi, L.M., Iaccarino, S., Mazzei, R., Salvatorini, G., Bambini, A.M., 2001. Il plancton calcareo (foraminiferi e nanoplancton) del Miocene delle Isole Tremiti. *Paleontogr. Ital.* 88, 64 pp.
- Fornaciari, E., Iaccarino, S., Mazzei, R., Rio, D., Salvatorini, G., Bossio, A., Monteforti, B., 1997. Calcareous plankton biostratigraphy of the Langhian historical stratotype. In: Montanari, A., Odin, G.S., Coccioni, R. (Eds.), Miocene Stratigraphy: An Integrated Approach. *Dev. Palaeontol. Stratigr.* 15, 89–96.
- Fornaciari, E., Di Stefano, A., Rio, D., Negri, A., 1996. Middle Miocene quantitative calcareous nanofossil biostratigraphy in the Mediterranean region. *Micropaleontology* 42, 37–63.
- Giannelli, L., Salvatorini, G., 1976. Due nuove specie di foraminiferi planctonici del Miocene. *Boll. Soc. Paleontol. Ital.* 15, 167–173.
- Hilgen, F.J., 1991a. Astronomical calibration of Gauss to Matuyama sapropels in the Mediterranean and implication for the Geomagnetic Polarity Time Scale. *Earth Planet. Sci. Lett.* 104, 226–244.
- Hilgen, F.J., 1991b. Extension of the astronomically calibrated (polarity) time scale to the Miocene/Pliocene boundary. *Earth Planet. Sci. Lett.* 107, 349–368.
- Hilgen, F.J., Iaccarino, S., Krijgsman, W., Montanari, A., Raffi, I., Turco, E., Zachariasse, W.J., 2003. The Global Stratotype Section and Point (GSSP) of the Tortonian Stage (Upper Miocene): a proposal.
- Hilgen, F.J., Krijgsman, W., Langereis, C.G., Lourens, L.J., Santarelli, A., Zachariasse, W.J., 1995. Extending the astronomical (polarity) time scale into the Miocene. *Earth Planet. Sci. Lett.* 136, 495–510.
- Hilgen, F.J., Krijgsman, W., Wijbrans, J.R., 1997. Direct comparison of astronomical and  $^{40}\text{Ar}/^{39}\text{Ar}$  ages of ash beds: potential implications for the age of mineral dating standards. *Geophys. Res. Lett.* 24, 2043–2046.
- Hilgen, F.J., Krijgsman, W., Raffi, I., Turco, E., Zachariasse, W.J., 2000a. Integrated stratigraphy and astronomical calibration of the Serravallian/Tortonian boundary section at Monte Gibliscemi, Sicily. *Mar. Micropaleontol.* 38, 181–211.
- Hilgen, F.J., Iaccarino, S., Krijgsman, W., Villa, G., Langereis, C.G., Zachariasse, W.J., 2000b. The global boundary stratotype section and point (GSSP) of the Messinian Stage (uppermost Miocene). *Episodes* 23, 172–178.
- Hilgen, F.J., Bissoli, L., Iaccarino, S., Krijgsman, W., Meijer, R., Negri, A., Villa, G., 2000c. Integrated stratigraphy and astrochronology of the Messinian GSSP at Oued Akrech (atlantic Morocco). *Earth Planet. Sci. Lett.* 182, 237–251.
- Iaccarino, S., 1985. Mediterranean Miocene and Pliocene planktic foraminifera. In: Bolli, H.M., Saunders, J.B., Perch-Nielsen, K. (Eds.), *Plankton Stratigraphy*. Cambridge University Press, pp. 283–314.
- Kennett, P.J., Srinivasan, M.S., 1983. *Neogene Planktonic Foraminifera: A Phylogenetic Atlas*. Hutchinson Ross Publishing Co., Stroudsburg, PA, 265 pp.
- Krijgsman, W., Hilgen, F.J., Langereis, C.G., Santarelli, A., Zachariasse, W.J., 1995. Late Miocene magnetostratigraphy, biostratigraphy and cyclostratigraphy from the Mediterranean. *Earth Planet. Sci. Lett.* 136, 475–494.
- Laskar, J., 1990. The chaotic motion of the solar system: A numerical estimate of the size of the chaotic zones. *Icarus* 88, 266–291.
- Laskar, J., Joutel, F., Boudin, F., 1993. Orbital, precessional, and insolation quantities for the Earth from –20 Myr to +10 Myr. *Astron. Astrophys.* 270, 522–533.
- Lirer, F., Caruso, A., Foresi, L.M., Sprovieri, M., Bonomo, S., Di Stefano, A., Di Stefano, E., Iaccarino, S.M., Salvatorini, G., Sprovieri, R., Mazzola, S., 2002. Astrochronological calibration of the upper Serravallian-lower Tortonian sedimentary sequence at Tremiti Islands (Adriatic Sea, Southern Italy). In: Iaccarino, S. (Ed.), *Integrated Stratigraphy and*

- Paleoceanography of the Mediterranean Middle Miocene. *Riv. Ital. Paleontol. Stratigr.* 108, 241–256.
- Lourens, L.J., Hilgen, F.J., Zachariasse, W.J., van Hoof, A.A.M., Antonarakou, A., Vergnaud-Grazzini, C., 1996. Evaluation of the Plio-Pleistocene astronomical time scale. *Paleoceanography* 11, 391–413.
- Lourens, L.J., Wehausen, R., Brumsack, H.J., 2001. Geological constraints on tidal dissipation and dynamical ellipticity of the Earth over the past three million years. *Nature* 409, 1029–1033.
- Montanari, A., Odin, G.S., Coccioni, R. (Eds.), 1997a. Miocene Stratigraphy. An Integrated Approach. *Dev. Palaeontol. Stratigr.* 15, 694 pp.
- Montanari, A., Beaudoin, B., Chan, L.S., Coccioni, R., Deino, A., De Paolo, D.J., Emmanuel, L., Fornaciari, E., Kruge, M., Lundblad, S., Mozzato, C., Portier, E., Renard, M., Rio, D., Sandroni, P., Stankiewicz, A., 1997b. Integrated stratigraphy of the Middle and Upper Miocene pelagic sequence of the Cònero Riviera (Marche region, Italy). In: Montanari, A., Odin, G.S., Coccioni, R. (Eds.), *Miocene Stratigraphy: An Integrated Approach*. *Dev. Palaeontol. Stratigr.* 15, 409–450.
- Odin, G.S., Montanari, A., Coccioni, R., 1997. Chronostratigraphy of Miocene stages: a proposal for the definition of precise boundaries. In: Montanari, A., Odin, G.S., Coccioni, R. (Eds.), *Miocene Stratigraphy: An Integrated Approach*. *Dev. Palaeontol. Stratigr.* 15, 597–629.
- Pälike, H., Shackleton, N.J., 2000. Constraints on astronomical parameters from the geological record for the last 25 Myr. *Earth Planet. Sci. Lett.* 182, 1–14.
- Prell, W.L., Kutzbach, J.E., 1987. Monsoon variability over the past 150,000 years. *J. Geophys. Res.* 92, 8411–8425.
- Raffi, I., Mozzato, C., Fornaciari, E., Hilgen, F.J., Rio, D., 2003. Late Miocene calcareous nannofossil biostratigraphy and astrochronology for the Mediterranean region. *Micropaleontology* 49, 1–26.
- Raffi, I., Rio, D., d'Atri, A., Fornaciari, E., Rocchetti, S., 1995. Quantitative distribution patterns and biomagnetostratigraphy of Middle to Late Miocene calcareous nannofossils from equatorial Indian and Pacific Oceans (Legs 115, 130, and 138). *Proc. ODP Sci. Results* 138, 479–502.
- Renne, P.R., Deino, A.L., Walter, R.C., Turrin, B.D., Swisher, C.C., Karner, D.B., Becker, T.A., Curtis, G.H., Sharp, W.D., Jaouni, A.R., 1994. Intercalibration of astronomical and radioisotopic time. *Geology* 22, 783–786.
- Renne, P.R., Swisher, C.C., Deino, A.L., Karner, D.B., Owens, T.L., DePaolo, D.J., 1998. Intercalibration of standards, absolute ages and uncertainties in  $^{40}\text{Ar}/^{39}\text{Ar}$  dating. *Chem. Geol.* 145, 117–152.
- Rosignol-Strick, M., 1983. African monsoons, an immediate climate response to orbital insolation. *Nature* 303, 46–49.
- Schmitz, M.D., Bowring, S.A., 2001. U-Pb zircon and titanite systematics of the Fish Canyon Tuff: an assessment of high-precision U-Pb geochronology and its application to young volcanic rocks. *Geochim. Cosmochim. Acta* 65, 2571–2587.
- Shackleton, N.J., Crowhurst, S., 1997. Sediment fluxes based on an orbitally tuned time scale 5 Ma to 14 Ma, Site 926. *Proc. ODP Sci. Results* 154, 69–82.
- Shackleton, N.J., Crowhurst, S.J., Weedon, G.P., Laskar, J., 1999. Astronomical calibration of Oligocene-Miocene time. *Phil. Trans. R. Soc. Lond. Ser. A* 357, 1907–1929.
- Sprovieri, R., di Stefano, E., Sprovieri, M., 1996. High resolution chronology for late Miocene Mediterranean stratigraphic events. *Riv. Ital. Paleontol. Stratigr.* 102, 77–104.
- Sprovieri, M., Caruso, A., Foresi, L.M., Bellanca, A., Neri, R., Mazzola, S., Sprovieri, R., 2002a. Astronomical calibration of the upper Langhian/lower Serravallian record of Ras Il-Pellegrin section (Malta Island, central Mediterranean). In: Iaccarino, S. (Ed.), *Integrated Stratigraphy and Paleoceanography of the Mediterranean Middle Miocene*. *Riv. Ital. Paleontol. Stratigr.* 108, 183–193.
- Sprovieri, R., Bonomo, S., Caruso, A., Di Stefano, A., Di Stefano, E., Foresi, L.M., Iaccarino, S.M., Lirer, F., Mazzei, R., Salvatorini, G., 2002b. Integrated calcareous plankton biostratigraphy and biochronology of the Mediterranean Middle Miocene. In: Iaccarino, S. (Ed.), *Integrated Stratigraphy and Paleoceanography of the Mediterranean Middle Miocene*. *Riv. Ital. Paleontol. Stratigr.* 108, 337–353.
- Steenbrink, J., van Vugt, N., Hilgen, F.J., Wijbrans, J.R., Meulenkamp, J.E., 1999. Sedimentary cycles and volcanic ash beds in the Lower Pliocene lacustrine succession of Ptolemais (NW Greece): discrepancy between  $^{40}\text{Ar}/^{39}\text{Ar}$  and astronomical ages. *Palaeogeogr. Palaeoclimat. Palaeoecol.* 152, 283–303.
- Tuenter, E., Weber, S.L., Hilgen, F.J., Lourens, L.J., 2003. The response of the African summer monsoon to remote and local forcing due to precession and obliquity. *Glob. Planet. Change* 36, 219–235.
- Turco, E., Hilgen, F.J., Lourens, L.J., Shackleton, N.J., Zachariasse, W.J., 2001. Punctuated evolution of global climate cooling during the late Middle to early Late Miocene High-resolution planktonic foraminiferal and oxygen isotope records from the Mediterranean. *Paleoceanography* 16, 405–423.
- Turco, E., Bambini, A.M., Foresi, L.M., Iaccarino, S., Lirer, F., Mazzei, R., Salvatorini, G., 2002. Middle Miocene high-resolution calcareous plankton biostratigraphy at Site 926 (Leg 154, equatorial Atlantic Ocean): paleoecological and paleobiogeographical implications. *Geobios* 35, 257–276.
- Zachariasse, W.J., 1992. Neogene planktonic foraminifers from Sites 761 and 762 off Northwest Australia. *Proc. ODP Sci. Results* 122, 665–675.